Birth, transition and maturation of canard cycles in a piecewise linear system with a flat slow manifold

V. Carmona* S. Fernández-García† A. E. Teruel‡

October 28, 2022

Abstract

In this work we deal with the canard regime as a part of a canard explosion taking place in a PWL version of the van der Pol equation having a flat critical manifold. The proposed analysis involves the identification of two specific canard cycles, one at the beginning and the other at the end of the canard regime, here called birth and maturation of canards, respectively. Moreover, inside the canard regime, we also analyse the transition from small amplitude canard cycles (canards without head) to large amplitude canard cycles (canards with head) by identifiying the maximal canard, transitory canard, and maximum period canard; and then proving that all these cycles are, in fact, different dynamical objects. There have been several works in the classical framework addressing the transitory regime, but from a numerical point of view. Some of these works involve systems exhibiting a flat slow manifold. The flat part of the nullcline implies a different transition from canard cycles without head to those with head than in the classical canard explosion. This is a good choice as a first approximation to the problem because, in particular, the different canard cycles appear further apart from one another. For that reason we have considered a four-zonal PWL system in which the critical manifold in the lateral left linear region is flat.

1 Introduction

Canard dynamics in slow-fast differential systems is characterised by the existence of orbits, named canard orbits, that after following an attracting manifold, then evolve close to a repelling manifold for a considerable amount of time. In the recent last years, this behaviour have been clearly identified in many applications. For example, canard orbits have been used to understand complex oscillations of both the bursting type, in excitable neurons, [33, 38], and the mixed mode type, in chemical reactions, [4, 13]. An interesting phenomenon associated with canard dynamics, is the so-called canard explosion, which consists of a sudden increase in the amplitude of an uniparametric family of limit cycles when the value of the parameter is slightly varied. This phenomenon explains the transient dynamics from small amplitude oscillations to relaxation oscillation taking place in the van der Pol oscillator, see [1, 16, 23].

Canard explosion is ubiquitous in planar slow-fast differential systems with a suitable fast nullcline [23], and it is a result of the interplay between the attracting and the repelling slow manifolds which appear as a consequence of the singular perturbation [17]. Accordingly, the canard regime is located in an exponentially small interval around the parameter value at which the attracting and repelling slow manifolds connect, giving rise to the so-called maximal trajectory.

Even when the canard dynamics has been widely studied, see [8, 40] and references therein, due inter alia to the extremely narrow interval where the canard regime occurs, some interesting challenges around the canard explosion are still not well understood. One of them consists in identifying the limit cycles acting as boundaries of the canard regime. The location of these canard cycles will help to a better understanding of both the transition from the small amplitude cycles, called the Hopf regime, to the canard regime, and especially the transition from the canard

MSC2010 subject classification: Primary: 34C05, 34C23, 34C25, 34E15, 34E17; Secondary: 37G15, 37G25.

Keywords: Piecewise linear systems, bifurcations, canards orbits, maximal canard, transitory canard.

*Dpto. Matemática Aplicada II & IMUS, University of Seville, Escuela Superior de Ingenieros, Avenida de los Descubrimientos s/n, 41092 Sevilla, Spain

†Dpto. EDAN & IMUS, University of Seville, Facultad de Matemáticas, C/ Tarfia, s/n., 41012 Sevilla, Spain. Corresponding author: soledad@us.es

‡Departament de Matemàtiques i Informàtica & IAC3, Universitat de les Illes Balears, Palma de Mallorca, Spain

regime to the relaxation regime. The transition from Hopf regime to canard regime is called the birth of canards, and the transition from the canard regime to the relaxation regime is called the maturation of canards.

Another of the challenges around the canard explosion is more related to the applications, in particular to the definition of excitability threshold in neural models. As it is well known, the FitzHugh-Nagumo (FHN) neural model [19, 28] does not have a well-defined excitability threshold, that is a value of the voltage beyond which a rapid increase of the membrane potential, that can be recognized as a spike, occurs [19]. Nevertheless, the presence of the canard explosion phenomenon in the FHN model allows to define a “quasi-threshold” through the repelling slow manifold. The strong divergence along this manifold transforms the canard cycle flowing along this slow manifold into a kind of separatrix, and hence, into a good candidate to define the “quasi-threshold” [39].

Some efforts to locate the canard cycle defining this “quasi-threshold” have been done by considering inflection sets [15] and exponential coordinate scaling [12], but also other canard cycles approximating it have been proposed: the maximal canard cycle, occuring when the attracting and the repelling slow manifolds do connect; the transitory canard cycle, which is the boundary between headless canard cycles and canard cycles with head; and the canard cycle having maximum period. However, all these canard cycles are not easy to be located and, indeed, it is not a well-known question whether all of them are different cycles or not. In [2] authors address a numerical study to locate all these canard cycles in the aircraft ground dynamics model [32], which is a slow-fast differential system exhibiting a flat critical manifold given by the graph of $y = -(x-a)e^{x/b}$, see Figure 1.

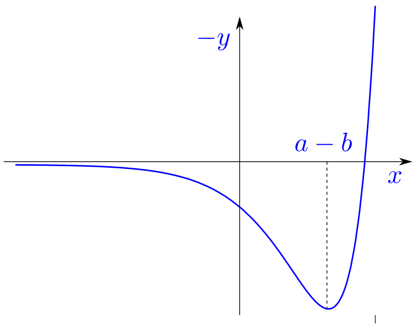

Figure 1: **Flat critical manifold.** Critical manifold $y = -(x-a)e^{x/b}$ of aircraft ground dynamics model [32] with $a > b > 0$ in the plane $(x, -y)$. The sign of the parameters is not relevant, the graph of the function can be brought to that of the figure by a suitable change of variables.

This critical manifold looks like a N-shaped curve in which one of the lateral branches has been flattened, which causes that the critical manifold loses the normal hyperbolicity at infinity. Hence, cycles of sufficiently large amplitude become relaxation oscillations. Moreover, large amplitude canard cycles appear further apart from one another than in systems with N-shaped fast nullcline. Consequently, slow-fast systems exhibiting flat slow manifold [3, 22, 24, 37] provide a good context for the analysis of the canard regime [2], in particular, for the analysis of the birth and the maturation of canards and for the definition of the quasy-threshold, that is, for the location of the maximal canard cycle, the transitory canard cycle [25] and the canard cycle with maximum period.

Recently, it has been understood how to reproduce aspects of the slow-fast dynamics in the context of piecewise linear (PWL) differential systems [9, 10, 11, 14, 18]. In particular, in [34] the authors show the existence of the canard explosion in the context of a PWL system of the FitzHugh-Nagumo type. More recently, in [5], we have analytically described the canard explosion after a Hopf-type bifurcation, both supercritical and subcritical, in a PWL generalized version of the FHN system, and provide accurate estimates for the parameter value for which the canard explosion occurs and for the amplitude and the period of the saddle-node canard cycles when they exist. In this previous version, the fast N-shaped nullcline is formed by a four-segment polygonal curve, so that three of these segments are used to define the fold around the point at which the Hopf bifurcation occurs. The width of this kink is of order $\sqrt{\varepsilon}$, so it tends to zero with ε, providing a critical N-shaped manifold.

Previous nullcline configuration has proven useful in the generation of the canard explosion. In particular, the three-segment fold provides the existence of the headless canard cycles, while the fourth segment defines a global return that enables the existence of the canard cycles with head and also of the relaxation cycles. Following this previous work, in the present manuscript we propose a PWL differential system with slow-fast dynamics exhibiting a fast nullcline which is a PWL version of the flat critical manifold in Figure 1. This approximation is obtained by concatenating three segments to define the fold and a horizontal one to define the flattened branch. The main aim of the paper is to locate, for the proposed system, the canard cycles both at the birth and at the maturation of the canards, together with the maximal canard cycle, the transitory canard cycle, the canard cycle with maximum period and the canard cycle through the repelling slow manifold, and to prove that all them are different canard cycles.

The rest of the article is organized as follows. In Section 2, we introduce the PWL differential system and the geometrical and dynamical basic elements which will be considered along the manuscript. After that, in Section 3 we establish the main results of the work. Then, we present the proofs of the main results in Section 4. Conclusions and perspectives are discussed in Section 5. Finally, the more technical questions are gathered in Appendices A and B.

2 Statement of the PWL system and its basic elements.

Here, we present the class of PWL systems that we aim to analyze, and also some geometric elements to describe the global dynamics. Moreover, we define some functions and quantities which are needed for stating the main results in the next section.

We consider the following slow-fast planar differential system,

$$\left\{ \begin{array}{l} x' = y - f(x,a,\varepsilon), \\ y' = \varepsilon(a - x), \end{array} \right. \tag{1}$$

with fast nullcline formed by three segments defining the fold and a horizontal one defining the flattened branch and given by

$$f(x,a,\varepsilon) = \left\{ \begin{array}{ll} 1 + \sqrt{\varepsilon}(a-1) + \varepsilon, & \text{if } x < -1 \\ -x + \sqrt{\varepsilon}(a-1) + \varepsilon, & \text{if } -1 < x \leqslant -\sqrt{\varepsilon}, \\ \sqrt{\varepsilon}(a-x), & \text{if } |x| \leqslant \sqrt{\varepsilon}, \\ x + \sqrt{\varepsilon}(a-1) - \varepsilon, & \text{if } x > \sqrt{\varepsilon}, \end{array} \right. \tag{2}$$

which is a piecewise linear version of the critical manifold depicted in Figure 1. The system depends on the two-dimensional parameter $\boldsymbol{\eta} = (a, \varepsilon) \in \mathbb{R}^2$, with $0 < \varepsilon \ll 1$.

The PWL character of the vector field allows the phase space to be divided into four regions: the lateral half-planes $\sigma_{LL} = \{(x,y) : x \leqslant -1\}$ and $\sigma_R = \{(x,y) : x \geqslant \sqrt{\varepsilon}\}$, and the central bands $\sigma_L = \{(x,y) : -1 \leqslant x \leqslant -\sqrt{\varepsilon}\}$ and $\sigma_C = \{(x,y) : |x| \leqslant \sqrt{\varepsilon}\}$, separated by the switching lines $x = -1$, $x = -\sqrt{\varepsilon}$ and $x = \sqrt{\varepsilon}$. Thus, restricted to the previous regions, the vector field is linear and can be expressed in a matrix way as $F_i(\mathbf{x}) = A_i\mathbf{x} + \mathbf{b}_i$ with $i \in \{LL, L, C, R\}$, being

$$A_{LL} = \begin{pmatrix} 0 & 1 \\ -\varepsilon & 0 \end{pmatrix}, \; A_L = \begin{pmatrix} 1 & 1 \\ -\varepsilon & 0 \end{pmatrix}, \; A_C = \begin{pmatrix} \sqrt{\varepsilon} & 1 \\ -\varepsilon & 0 \end{pmatrix}, \; A_R = \begin{pmatrix} -1 & 1 \\ -\varepsilon & 0 \end{pmatrix},$$

$$\mathbf{b}_{LL} = \begin{pmatrix} -1 - \sqrt{\varepsilon}(a-1) - \varepsilon \\ \varepsilon a \end{pmatrix}, \; \mathbf{b}_L = \begin{pmatrix} -\sqrt{\varepsilon}(a-1) - \varepsilon \\ \varepsilon a \end{pmatrix}, \; \mathbf{b}_C = \begin{pmatrix} -\sqrt{\varepsilon}a \\ \varepsilon a \end{pmatrix},$$

and

$$\mathbf{b}_R = \begin{pmatrix} -\sqrt{\varepsilon}(a-1) + \varepsilon \\ \varepsilon a \end{pmatrix}.$$

The local behavior of the flow of system (1) at any of the regions σ_i with $i \in \{LL, L, C, R\}$ is determined by the trace t_i and the determinant $d_i = \varepsilon$ of the matrix A_i through the discriminant $\Delta_i = t_i^2 - 4\varepsilon$, the eigenvalues λ_i^s and λ_i^q, the eigenvectors $\mathbf{v}_i^s = (\lambda_i^s, -\varepsilon)^T$ and $\mathbf{v}_i^q = (\lambda_i^q, -\varepsilon)^T$, and the location of the points $\mathbf{e}_i = -A_i^{-1}\mathbf{b}_i$. All these elements are given by:

$$\begin{array}{llll} t_{LL} = 0, & t_L = 1, & t_C = \sqrt{\varepsilon}, & t_R = -1, \\ \Delta_{LL} = -4\varepsilon, & \Delta_L = 1 - 4\varepsilon, & \Delta_C = -3\varepsilon, & \Delta_R = 1 - 4\varepsilon, \\ \lambda_{LL}^s = -\sqrt{\varepsilon}i, & \lambda_L^s = \frac{1-\sqrt{1-4\varepsilon}}{2}, & \lambda_C^s = \frac{\sqrt{\varepsilon}(1-\sqrt{3}i)}{2}, & \lambda_R^s = \frac{-1+\sqrt{1-4\varepsilon}}{2}, \\ \lambda_{LL}^q = \sqrt{\varepsilon}i & \lambda_L^q = 1 - \lambda_L^s, & \lambda_C^q = \frac{\sqrt{\varepsilon}(1+\sqrt{3}i)}{2}, & \lambda_R^q = -1 - \lambda_R^s, \end{array} \tag{3}$$

and

$$\mathbf{e}_{LL} = \begin{pmatrix} a \\ 1+\sqrt{\varepsilon}(a-1)+\varepsilon \end{pmatrix}, \quad \mathbf{e}_L = \begin{pmatrix} a \\ -a+\sqrt{\varepsilon}(a-1)+\varepsilon \end{pmatrix},$$
$$\mathbf{e}_R = \begin{pmatrix} a \\ a+\sqrt{\varepsilon}(a-1)-\varepsilon \end{pmatrix}, \qquad \mathbf{e}_C = \begin{pmatrix} a \\ 0 \end{pmatrix}. \tag{4}$$

Note that λ_L^s and λ_R^s are of order 1 in ε while λ_L^q and λ_R^q are of order 0 in ε, implying a slow-fast splitting of the dynamics in the σ_L and σ_R regions. On the contrary, eigenvalues $\lambda_{LL}^s, \lambda_{LL}^q, \lambda_C^s$, and λ_C^q are of order $\frac{1}{2}$ in ε impliying no slow-fast splitting in σ_{LL} and σ_C. Moreover, notice that, $\mathbf{e}_i$ is an equilibrium point only when $\mathbf{e}_i \in \sigma_i$. Otherwise, these points are called *virtual equilibrium points*, and even when they are not equilibrium points, they organise the dynamic behaviour of the system in their corresponding region σ_i.

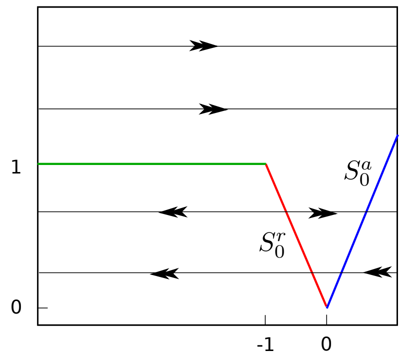

Figure 2: **Flat critical manifold S_0 of system** (1). This is a PWL version of the critical curve shown in Figure 1. The layer flow of the fast subsystem of system (1) is also represented. The segment S_0^r and the half-line S_0^a are, respectively, the repelling and the attracting branches of the critical manifold.

The critical manifold S_0, formed by the equilibria of the fast subsystem of system (1) when $\varepsilon = 0$, is given by the graph of the PWL function $y = f(x, a, 0)$. It is a normally hyperbolic manifold, except at the horizontal half-line, that is for $x \in (-\infty, -1]$, and at the origin $(0, 0)$. The segment S_0^r defined for $x \in (-1, 0)$ is the repelling branch, and the half-line S_0^a defined for $x > 0$ is the attracting branch, see Figure 2. From Lemma 4 in [31], the slow manifold S_ε of system (1), with $0 < \varepsilon \ll 1$, is locally formed by segments, each of them contained in a region σ_L, σ_R and defined by the slow eigenvector $\mathbf{v}_i^s = (\lambda_i^s, -\varepsilon)^T$ associated to the slow eigenvalue λ_i^s with $i \in \{L, R\}$. Then,

$$S_\varepsilon = \begin{cases} S_\varepsilon^r = \mathbf{e}_L - r\mathbf{v}_L^s & r \in \left[\frac{\sqrt{\varepsilon}+a}{\lambda_L^s}, \frac{1+a}{\lambda_L^s}\right], \\ S_\varepsilon^a = \mathbf{e}_R - r\mathbf{v}_R^s & r \in \left[\frac{a-\sqrt{\varepsilon}}{\lambda_R^s}, +\infty\right). \end{cases} \tag{5}$$

We conclude that S_ε^a and S_ε^r are the attracting branch and the repelling branch, respectively, of a canonical slow manifold S_ε, see Figure 3. Moreover, since the horizontal half-line of the critical manifold is not normally hyperbolic, no piece of the slow manifold is located in the region σ_{LL}. Finally, since in σ_C there is no real separation between fast and slow behaviour at the eigenvalues level, it follows that there is no branch of the slow manifold, neither attracting nor repelling, which is contained in this region. This observation was firstly commented in [11] where, when no other repelling slow manifold does exist, cycles flowing along this region are called quasi-canards.

According to expression (5), the attracting branch S_ε^a intersects with the switching line $x = \sqrt{\varepsilon}$ at the point

$$\mathbf{q}_1^R = \begin{pmatrix} \sqrt{\varepsilon} \\ (\lambda_R^s - \sqrt{\varepsilon})(\sqrt{\varepsilon} - a) \end{pmatrix}, \tag{6}$$

whereas the repelling branch S_ε^r intersects the switching lines $x = -1$ and $x = -\sqrt{\varepsilon}$ at the points

$$\mathbf{q}_1^L = \begin{pmatrix} -1 \\ (\sqrt{\varepsilon}-1)(\sqrt{\varepsilon}+a) + (1+a)\lambda_L^q \end{pmatrix}, \quad \mathbf{q}_0^L = \begin{pmatrix} -\sqrt{\varepsilon} \\ (\sqrt{\varepsilon} - \lambda_L^s)(\sqrt{\varepsilon}+a) \end{pmatrix}, \tag{7}$$

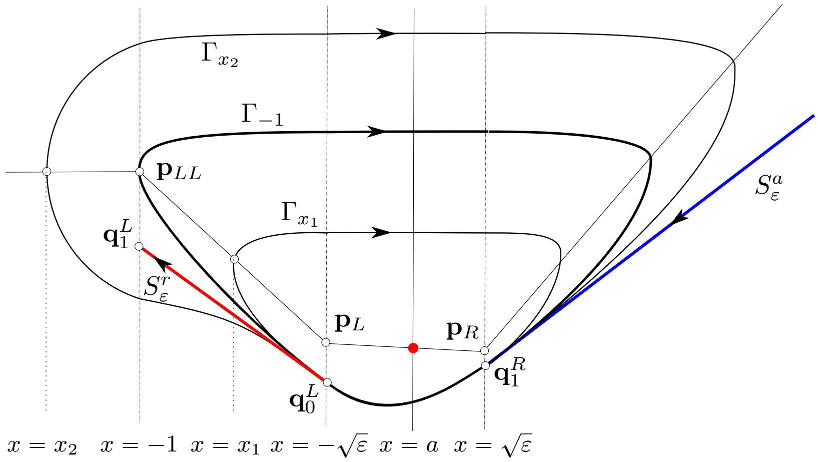

Figure 3: **Geometrical and dynamical key elements for $|a| \leqslant \sqrt{\varepsilon}$.** x-nullcline and intersection points $\mathbf{p}_{LL}$, $\mathbf{p}_L$ and $\mathbf{p}_R$ with the switching lines. Attracting S_ε^a and repelling S_ε^r canonical slow manifolds and intersection points $\mathbf{q}_1^R$, $\mathbf{q}_0^L$ and $\mathbf{q}_1^L$ with the switching lines. Headless canard cycle Γ_{x_1}, transitory canard cycle Γ_{-1} and canard cycle with head Γ_{x_2}.

respectively, see Figure 3. We also highlight the intersection points of the x-nullcline of system (1) with the switching lines $x = -1, x = -\sqrt{\varepsilon}$ and $x = \sqrt{\varepsilon}$,

$$\mathbf{p}_{LL} = \begin{pmatrix} -1 \\ 1 + \sqrt{\varepsilon}(a-1) + \varepsilon \end{pmatrix}, \quad \mathbf{p}_L = \begin{pmatrix} -\sqrt{\varepsilon} \\ \sqrt{\varepsilon}(\sqrt{\varepsilon} + a) \end{pmatrix} \quad \text{and} \quad \mathbf{p}_R = \begin{pmatrix} \sqrt{\varepsilon} \\ \sqrt{\varepsilon}(a - \sqrt{\varepsilon}) \end{pmatrix}, \tag{8}$$

respectively. Note that the flow of system (1) at these points is tangent to the switching lines.

Regarding the limit cycles of system (1), we note that every limit cycle Γ intersects the x-nullcline $y = f(x, a, \varepsilon)$ at exactly one point $(x, f(x, a, \varepsilon))$ having the property $x < a$. From now on, we call *width of the limit cycle* Γ, to the first coordinate of this intersection point and we use it to identify the limit cycle. Therefore, the limit cycle Γ_x will be the limit cycle having width equal to x, see Figure 3 for $x = x_1$ and $x = x_2$.

Due to the free divergence ($t_{LL} = 0$) in the zone σ_{LL}, the dynamics in this region is of center type and, restricted to σ_{LL}, the function $H_{LL}(x, y) = \varepsilon(x-a)^2 + (y-p_2)^2$ is constant on the orbits, where p_2 is the second coordinate of point $\mathbf{p}_{LL}$ given in (8). Hence, given a limit cycle Γ_x of width $x < -1$, the intersection points $(-1, y_x^\pm)$ of Γ_x with the switching line $\{x = -1\}$ are symetrically located on either sides of $\mathbf{p}_{LL}$, that is, $y_x^\pm = p_2 \pm d$, where the distance d satisfies the relationship $H_{LL}(-1, p_2 - d) = H_{LL}(x, p_2)$ and hence,

$$x = -\frac{\sqrt{d^2 + (a+1)^2\varepsilon} - a\sqrt{\varepsilon}}{\sqrt{\varepsilon}} \qquad \text{and} \qquad d = \sqrt{\varepsilon}\sqrt{(x+1)(x-1-2a)}. \tag{9}$$

Consider system (1) with $a < \sqrt{\varepsilon}$, which implies that the equilibrium of the system does not belong to the region σ_R. The center dynamics in the left region σ_{LL}, the repelling dynamics in σ_L, and the focus behaviour in σ_C together with the attracting slow manifold S_ε^a in the right region σ_R, allow us to assure that the positive semi-orbit through a point $(x, f(x, a, \varepsilon))$, with $x < a$, intersects the nullcline in a point $(x_1, f(x_1, a, \varepsilon))$, with $x_1 < a$. This fact lets us define the Poincaré map as follows.

Definition 2.1 *Consider $\varepsilon_0 > 0$ small enough. We define the image of (x, a, ε) by the Poincaré map $\Pi : (-\infty, a) \times (-\infty, \sqrt{\varepsilon}) \times (0, \varepsilon_0) \to (-\infty, a)$ as the first coordinate of the next intersection point $(x_1, f(x_1, a, \varepsilon))$ with $x_1 < a$, between the $x-$nullcline and the positive semi-orbit passing through the point $(x, f(x, a, \varepsilon))$.*

Associated to each limit cycle Γ_x, we can define the following times of flight, as follows.

Definition 2.2 *For $\varepsilon > 0$, consider a limit cycle Γ_x. We define the period $T(x, a, \varepsilon)$ of Γ_x as the time spent by the orbit from the point $(x, f(x, a, \varepsilon))$ to the point $(\Pi(x, a, \varepsilon), f(\Pi(x, a, \varepsilon), a, \varepsilon))$. Then, the period $T(x, a, \varepsilon)$ can be descomposed as the sum of the times of flight τ_i that the limit cycle spends in each zone σ_i, with $i \in \{LL, L, C, R\}$, that is*

$$T(x, a, \varepsilon) = \tau_{LL} + \tau_L + \tau_C + \tau_R.$$

One special limit cycle, assuming that it exists, is the one having width $x = -1$. Such a limit cycle is tangent to the switching line $\{x = -1\}$ at the point $\mathbf{p}_{LL}$, and therefore, it is the separation cycle between the limit cycles intersecting the lateral region σ_{LL} and those that do not intersect it, see Γ_{-1} in Figure 3. In a similar way, the limit cycle having width $x = -\sqrt{\varepsilon}$ is tangent at $\mathbf{p}_L$ to the switching line $\{x = -\sqrt{\varepsilon}\}$ and it is the separation cycle between the limit cycles intersecting the region σ_L and those that do not intersect it.

When ε is small enough, the limit cycles with width $-1 < x < -\sqrt{\varepsilon}$ will be referred to as *headless canard limit cycles* whereas limit cycles with width $x < -1$ will be referred to as *canard limit cycles with head*. Therefore, the limit cycle with width $x = -1$ will be referred to as *the transitory canard*, see [27], and it is the boundary between headless canard cycles and canard cycles with head.

3 Statement of the Main Results

In this section, we present the main results in the paper. These results regarding the existence of a one parameter family of stable limit cycles in the PWL system (1) borning at a Hopf-like bifurcation, and to the description about how the amplitudes of the cycles in the family evolve.

In the first result we assure that, the starting point of the curve organizing the family of limit cycles exhibited by system (1) takes place at a Hopf-like bifurcation [20, 21, 35, 36]. At this bifurcation, a limit cycle appears after the change of stability of the equilibrium point, just like in the Hopf bifurcation. The difference between both kind of bifurcations is the relation between the amplitude of the limit cycle and the value of the bifurcation parameter. This relation is linear in the Hopf-like bifurcation and a square root in the Hopf bifurcation.

Since the Hopf-like bifurcation is a local phenomenon, involving only two regions of linearity, the following result can be derived from Theorem 5 in [20]. See also Theorem 5.1 and Theorem 5.2 in [36], or Theorem 4.1 in [5] in the particular case $m = -\sqrt{\varepsilon}$ and $k = 1$.

Theorem 3.1 (Hopf-like bifurcation) *System* (1) *has a unique equilibrium point* $\mathbf{e} = (a, f(a))$, *which converges to the fold of the critical manifold at the origin as* (ε, a) *tends to* $(0, 0)$*. Moreover, the equilibrium point* $\mathbf{e}$ *is asymptotically stable for* $a > \sqrt{\varepsilon}$ *and looses stability through a Hopf-like bifurcation across* $a = \sqrt{\varepsilon}$*. In particular, when* $\varepsilon > 0$ *is sufficiently small, a stable limit cycle appears in a supercritical bifurcation for* $a < \sqrt{\varepsilon}$*, and the size of the limit cycle depends linearly on the distance* $|\sqrt{\varepsilon} - a|$.

In the next result, we study the possibility of connecting the point $\mathbf{q}_1^R$ with a given point $\mathbf{p}_0$ of the switching line $\{x = -\sqrt{\varepsilon}\}$ through an orbit of the system in the central region σ_C. The point $\mathbf{p}_0$ can be written in the form

$$\mathbf{p}_0 = \mathbf{q}_L^0 + Y\varepsilon^{3/2}(0, 1)^T, \tag{10}$$

with $-\infty \leqslant Y \leqslant \widetilde{Y}_0$, being

$$\widetilde{Y}_0 = \frac{\sqrt{\varepsilon} + a}{\lambda_L^q \sqrt{\varepsilon}}. \tag{11}$$

We note that when $Y = \widetilde{Y}_0$ the point $\mathbf{p}_0$ coincides with the point $\mathbf{p}_L$, at which the flow is tangent to $\{x = -\sqrt{\varepsilon}\}$ and this value is, hence, the limit of the region where the orbits cross from the central region σ_C to the region σ_L. On the other hand, when Y vanishes the point $\mathbf{p}_0$ coincides with $\mathbf{q}_L^0$, which implies that both branches of the slow manifold, S_ε^a and S_ε^r, connect giving rise to the maximal trajectory, see Figure 3.

Theorem 3.2 (Connection near the slow manifold) *Let us consider the values* $\mathbf{q}_1^R$, $\mathbf{q}_0^L$, *and* $\widetilde{Y}_0$ *given in* (6)*,* (7)*, and* (11)*, respectively. Let us define*

$$\widetilde{Y}_0^* = \frac{2e^{\frac{\pi}{\sqrt{3}}}}{1 + e^{\frac{\pi}{\sqrt{3}}}} \tag{12}$$

and let us fix a value $Y_0 \in \left(-\infty, \widetilde{Y}_0^*\right)$*. Then, there exist a value* $0 < \mu \ll 1$ *and two analytic functions* A_S *and* η_S *defined in* $U = (Y_0 - \mu, Y_0 + \mu) \times (-\mu, \mu)$ *such that if* $0 < \varepsilon < \mu^2$ *and* $a = a_S(Y, \varepsilon) := \sqrt{\varepsilon} A_S(Y, \sqrt{\varepsilon})$*, then the orbit of system* (1) *starting in point* $\mathbf{q}_1^R$ *reaches the switching line* $\{x = -\sqrt{\varepsilon}\}$ *at the point* $\mathbf{p}_0 = \mathbf{q}_0^L + Y\varepsilon^{3/2}(0, 1)^T$ *with the time of flight* $\tau_C^S(Y, \varepsilon) :=$

$\eta_S(Y,\sqrt{\varepsilon})/\sqrt{\varepsilon}>0$. *In addition, the first terms of the expansions of* a_S *and* τ_C^S *in terms of* $\sqrt{\varepsilon}$ *are given by*

$$a_S(Y,\varepsilon)=\frac{e^{\frac{\pi}{\sqrt{3}}}-1}{e^{\frac{\pi}{\sqrt{3}}}+1}\sqrt{\varepsilon}-\frac{C(Y)\,Y}{4e^{\frac{\pi}{\sqrt{3}}}\left(e^{\frac{\pi}{\sqrt{3}}}+1\right)}\varepsilon^{\frac{3}{2}}+O(\varepsilon^2) \tag{13}$$

and

$$\tau_C^S(Y,\varepsilon)=\frac{2\pi}{\sqrt{3}\sqrt{\varepsilon}}+\frac{C(Y)}{2e^{\frac{\pi}{\sqrt{3}}}}-\frac{\left(e^{\frac{\pi}{\sqrt{3}}}+1\right)C(Y)\,Y}{8e^{\frac{2\pi}{\sqrt{3}}}}\sqrt{\varepsilon}+O(\varepsilon), \tag{14}$$

where

$$C(Y)=(e^{\frac{\pi}{\sqrt{3}}}+1)Y-4e^{\frac{\pi}{\sqrt{3}}}. \tag{15}$$

Notice that the existence of the functions $a_S(0,\varepsilon)$ and $\tau_C^S(0,\varepsilon)$ which guarantee the connection of both branches of the slow manifold when $Y=0$, were derived in [5, Theorem 3.2]. Here, considering that Y does not vanish, we have extended the existence to a neighbourhood of the slow manifold.

The existence of the connection between the attracting and repelling slow manifolds, together with the free divergence character of the flow in the region σ_{LL}, allow for a global return of the flow, which provides the arguments to establish the following result about the existence of cycles of any suitable width. To state the result in a proper way, we introduce the following values corresponding with the end points of the canard regime, see Lemma 4.1 in Subsection 4.2

$$\begin{aligned} x_r(\varepsilon)&=-\frac{\sqrt{\lambda_L^q\left(1-\sqrt{\varepsilon}\left(1+\frac{1}{|\ln(\varepsilon)|}\right)\right)^2+\lambda_L^s(1+\tilde{a})^2}}{\sqrt{\lambda_L^s}}+\tilde{a}=-\frac{1}{\sqrt{\varepsilon}}+1+O(\varepsilon^{1/2}),\\ x_s(\varepsilon)&=-\sqrt{\varepsilon}-\frac{1}{|\ln(\varepsilon)|}(\sqrt{\varepsilon}+\tilde{a}), \end{aligned} \tag{16}$$

where $\tilde{a}=a_S(0,\varepsilon)$ in order to simplify notations. Moreover, when no confusion arises we remove the ε dependency on $x_r(\varepsilon)$ and $x_s(\varepsilon)$.

Theorem 3.3 (Existence of canard limit cycles) *Consider* $\varepsilon_0>0$ *small enough and* $x_0\in(-\infty,x_s(\varepsilon_0))$. *There exists a* $\mathcal{C}^\infty$*-function* A_N *defined in* $U=(x_0-\mu,x_0+\mu)\times(-\sqrt{\mu},\sqrt{\mu})$ *with* $0<\mu\ll 1$, *such that if* $0<\varepsilon<\mu$, *system* (1) *with* $a=a_N(x,\varepsilon):=\sqrt{\varepsilon}A_N(x,\sqrt{\varepsilon})$ *possesses a stable limit cycle,* Γ_x, *passing through* $(x,f(x))$. *Moreover, if* $x_0\in(x_r(\varepsilon),x_s(\varepsilon))$, *function* $a_N(x_0,\varepsilon)$ *has the same Taylor series expansion in* $\sqrt{\varepsilon}$ *as* $a_S(0,\varepsilon)$, *with* a_S *given in Theorem 3.2, and therefore,* Γ_{x_0} *is a canard cycle. Furthermore, if* $x_0\in(-1,x_s(\varepsilon))$, *then* Γ_{x_0} *is a headless canard; and if* $x_0\in(x_r(\varepsilon),-1)$, *then* Γ_{x_0} *is a canard with head. Finally, if* $x_0\in(-\infty,x_r(\varepsilon)]$, *then* Γ_{x_0} *is a relaxation oscillation.*

The above theorem describes the family of limit cycles depending on width of the cycles, and assures for this family the existence of the canard explosion restricted to the interval (x_r,x_s), since every cycle Γ_x with $x\in(x_r,x_s)$ occurs for a parameter value $a=a_N(x,\varepsilon)$ having the same Taylor series expansion in $\sqrt{\varepsilon}$ than $a_S(0,\varepsilon)$. Moreover, limit cycles having width $x<x_r$ are relaxation oscillations, whereas limit cycles having width $x_s<x<-\sqrt{\varepsilon}$ are still under the effect of the Hopf-like bifurcation, namely, the Hopf regime.

In the next result, we provide information about the period function $T(x,\varepsilon)=T(x,a_N(x,\varepsilon),\varepsilon)$ of canard cycles in terms of the width x.

Theorem 3.4 (Properties of period function) *Set* ε_0 *sufficiently small. There exists a function* $T:U=(-\infty,x_s(\varepsilon_0))\times(0,\varepsilon_0)\to\mathbb{R}^+$, *function of* $(x,\sqrt{\varepsilon})$ *such that* $T(x,\varepsilon)$ *is the period of the cycle* Γ_x *whose existence has been established in Theorem 3.3 for the parameter* $a=a_N(x,\varepsilon)$. *Moreover, the following statements hold.*

a) There exists a function $x_P(\varepsilon)$, $\mathcal{C}^\infty$ *as a function of* $\varepsilon^{1/3}$, *defined in* $(0,\varepsilon_0)$ *which provides the maximum of the period* T, *that is*

$$\frac{\partial T}{\partial x}(x,\varepsilon)>0,\ x\in(x_r,x_P(\varepsilon)),\quad \frac{\partial T}{\partial x}(x_P(\varepsilon),\varepsilon)=0,\quad \frac{\partial T}{\partial x}(x,\varepsilon)<0,\ x\in(x_P(\varepsilon),x_s).$$

b) The maximum satisfies that

$$x_P(\varepsilon) = -\varepsilon^{-1/6} + O(\varepsilon^{1/2}),$$

$$T(x_P(\varepsilon), \varepsilon) = \frac{1}{\varepsilon} \ln \left(\frac{C_0(1-\varepsilon^{\frac{2}{3}})}{\varepsilon} \right) + O(\varepsilon^{-\frac{1}{2}}),$$

where,

$$C_0 = \frac{(1+e^{\frac{\pi}{\sqrt{3}}})^2}{4e^{\frac{\pi}{\sqrt{3}}}}.$$

We recall that $x = -1$ is the width of the transitory canard cycle Γ_{-1}, that is, the one at the boundary between headless canard cycles and canard cycles with head. Let $\widetilde{x}(\varepsilon)$ and $x_M(\varepsilon)$ be the width of, respectively, $\Gamma_{\widetilde{x}}$ the canard cycle through the point $\mathbf{q}_1^L$, i.e, the one passing through the repelling branch of the slow manifold, and Γ_{x_M} the maximal canard cycle, that is the one obtained just when both branches of the slow manifold coincide. In the next theorem we establish the order of the width of all these canard cycles which are depicted in Figure 4.

Theorem 3.5 (Order of canard limit cycles) *Set $\varepsilon_0 > 0$ sufficiently small. Transitory canard Γ_{-1}, maximal canard Γ_{x_M} and the canard with maximal period Γ_{x_P} are ordered as follows,*

$$x_r < x_P < \widetilde{x} < x_M \leqslant -1 < x_s.$$

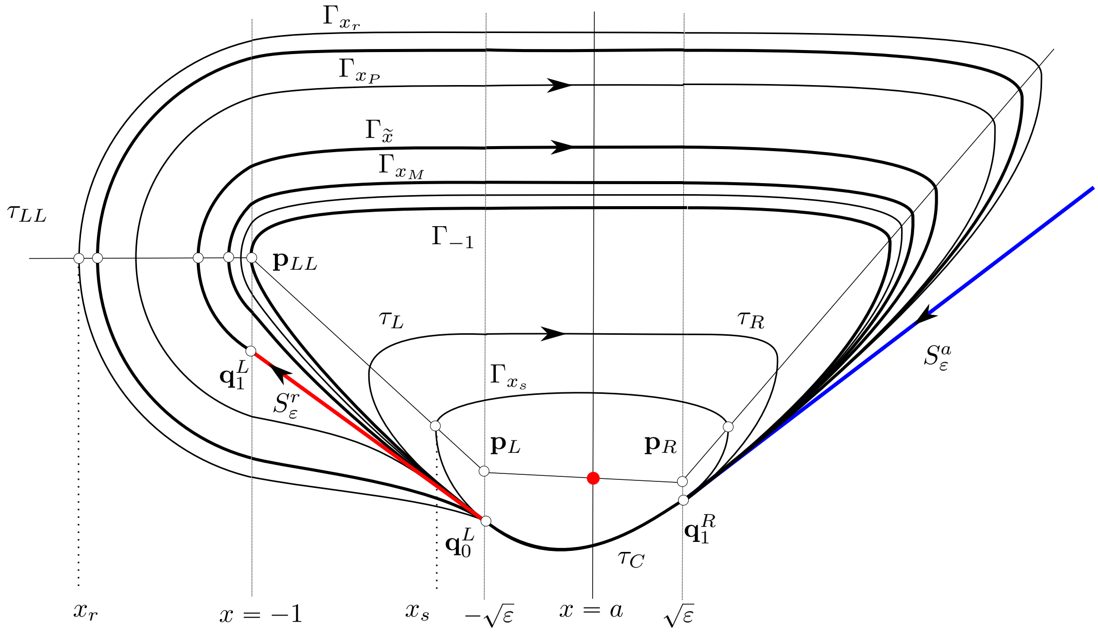

Figure 4: **Canard regime: from birth to maturation.** The birth of canards occurs at cycle Γ_{x_s}, whereas the maturation at Γ_{x_r}. The transition from headless canard cycles to canard cycles with head at the transitory canard Γ_{-1}, maximal canard Γ_{x_M} taking place at the conection between the slow-manifolds, canard cycle through the repelling slow manifold $\Gamma_{\widetilde{x}}$ and the maximum period canard cycle Γ_{x_P}.

4 Proofs of the Main Results

4.1 Proof of Theorem 3.2

As a first step, a direct computation shows that the orbit of the linear differential system

$$\begin{cases} x' = y - \sqrt{\varepsilon}(a - x), \\ y' = \varepsilon(a - x), \end{cases}$$

passing through the point $\mathbf{q}_1^R$ can be parametrized as $(x(t;a,\varepsilon), y(t;a,\varepsilon))$, where

$$\begin{aligned} x_C(t;a,\varepsilon) &= \tfrac{1}{3\sqrt{\varepsilon}}\left(\sqrt{\varepsilon}-a\right)e^{\frac{t\sqrt{\varepsilon}}{2}}\left(\sqrt{3}\left(\sqrt{1-4\varepsilon}-\sqrt{\varepsilon}-1\right)\sin\left(\sqrt{3\varepsilon}\,t/2\right)+3\sqrt{\varepsilon}\cos\left(\sqrt{3\varepsilon}\,t/2\right)\right)+a,\\ y_C(t;a,\varepsilon) &= -\tfrac{1}{6}\left(\sqrt{\varepsilon}-a\right)e^{\frac{t\sqrt{\varepsilon}}{2}}\left(\sqrt{3}\left(\sqrt{1-4\varepsilon}+2\sqrt{\varepsilon}-1\right)\sin\left(\sqrt{3\varepsilon}\,t/2\right)+\right.\\ &\quad \left.\left(-3\sqrt{1-4\varepsilon}+6\sqrt{\varepsilon}+3\right)\cos\left(\sqrt{3\varepsilon}\,t/2\right)\right) \end{aligned}$$

with $t \in \mathbb{R}$.

Now, we want to find two values $\tau_C^S > 0$ and $a_S \in \mathbb{R}$, depending on $\varepsilon > 0$ and Y_0, such that

$$\begin{aligned} &F_1(\tau_C^S, a_S, \varepsilon) = 0,\\ &F_2(\tau_C^S, a_S, \varepsilon, Y_0) = 0,\\ &|x_C(\tau; a_S, \varepsilon)| < \sqrt{\varepsilon}, \quad \text{for} \quad \tau \in (0, \tau_C^S), \end{aligned} \tag{17}$$

where

$$F_1(\tau, a, \varepsilon) = x(\tau; a, \varepsilon) + \sqrt{\varepsilon} \tag{18}$$

and

$$F_2(\tau, a, \varepsilon, Y_0) = y(\tau; a, \varepsilon) - \left(\sqrt{\varepsilon} - \lambda_L^s\right)\left(\sqrt{\varepsilon} + a\right) - Y_0\,\varepsilon^{3/2}. \tag{19}$$

Notice that the two first equations of (17) imply that the orbit reaches the point $\mathbf{q}_0^L + Y_0\,\varepsilon^{3/2}\mathbf{e}_2$ and the last inequality assures that the orbit remains in the zone σ_C for $\tau \in (0, \tau_C^S)$.

Next, we deal with the solutions of the nonlinear system of two equations $F_1(\tau, a, \varepsilon) = 0$, $F_2(\tau, a, \varepsilon, Y) = 0$ and four unknowns $(\tau, a, \varepsilon, Y)$. After that, we will check that the solutions found also satisfy the inequality in (17).

The change of variable

$$(\tau, a, \varepsilon, Y) = \left(\eta\delta^{-1}, A\delta, \delta^2, Y\right), \tag{20}$$

valid for $\varepsilon, \delta > 0$, allows to write the system $F_1 = 0$ and $F_2 = 0$ into the form $\delta G_1(\eta, A, \delta) = 0$ and $\delta^2 G_2(\eta, A, \delta, Y) = 0$, where

$$G_1(\eta, A, \delta) = \frac{1-A}{\sqrt{3}}e^{\eta/2}\left(\sqrt{3}\cos\left(\sqrt{3}\,\eta/2\right) - \left(\frac{4\delta}{\sqrt{1-4\delta^2}+1}+1\right)\sin\left(\sqrt{3}\,\eta/2\right)\right) + A + 1 \tag{21}$$

and

$$\begin{aligned} G_2(\eta, A, \delta, Y) = {}& \frac{A-1}{\sqrt{3}}e^{\eta/2}\left(\sqrt{3}\left(\frac{2\delta}{\sqrt{1-4\delta^2}+1}+1\right)\cos\left(\sqrt{3}\,\eta/2\right) + \left(1 - \frac{2\delta}{\sqrt{1-4\delta^2}+1}\right)\sin\left(\sqrt{3}\,\eta/2\right)\right) - \\ & (A+1)\left(1 - \frac{2\delta}{\sqrt{1-4\delta^2}+1}\right) - Y\delta. \end{aligned} \tag{22}$$

Since systems $(F_1, F_2) = (0, 0)$ and $(G_1, G_2) = (0, 0)$ are equivalent for $\delta = \sqrt{\varepsilon} > 0$, from now on we will find solutions for the second one.

From straightforward computations it follows that the point

$$(\eta_0, A_0, \delta_0, Y_0) = \left(\frac{2\pi}{\sqrt{3}}, \frac{e^{\frac{\pi}{\sqrt{3}}}-1}{e^{\frac{\pi}{\sqrt{3}}}+1}, 0, Y_0\right)$$

is a solution of system $(G_1, G_2) = (0, 0)$. Since the determinant of the Jacobian matrix is

$$\det\left(D_{\eta,A}G(\eta_0, A_0, \delta_0, Y_0)\right) = \begin{pmatrix} \dfrac{\partial G_1}{\partial \eta}(\eta_0, A_0, \delta_0) & \dfrac{\partial G_1}{\partial A}(\eta_0, A_0, \delta_0) \\ \dfrac{\partial G_2}{\partial \eta}(\eta_0, A_0, \delta_0, Y_0) & \dfrac{\partial G_2}{\partial A}(\eta_0, A_0, \delta_0, Y_0) \end{pmatrix} = -2e^{\frac{\pi}{\sqrt{3}}} \neq 0,$$

the Implicit Function Theorem assures that there exists a value $\mu := \mu(Y_0) > 0$ and two analytic functions η_S and A_S defined in $(Y_0 - \mu, Y_0 + \mu) \times (-\mu, \mu)$ such that $\eta_S(Y_0, 0) = \eta_0$, $A_S(Y_0, 0) = A_0$ and $G_1\left(\eta_S(Y, \delta), A_S(Y, \delta), \delta\right) = G_2\left(\eta_S(Y, \delta), A_S(Y, \delta), \delta, Y\right) = 0$ for all $(Y, \delta) \in (Y_0 - \mu, Y_0 + \mu) \times (-\mu, \mu)$. Moreover, after some direct calculations, one can see that the functions η_S and A_S can be written as

$$\eta_S(Y, \delta) = \frac{2\pi}{\sqrt{3}} + \frac{C(Y)}{2e^{\frac{\pi}{\sqrt{3}}}}\delta - \frac{\left(e^{\frac{\pi}{\sqrt{3}}}+1\right)C(Y)\,Y}{8e^{\frac{2\pi}{\sqrt{3}}}}\delta^2 + O(\delta^3)$$

and

$$A_S(Y,\delta) = \frac{e^{\frac{\pi}{\sqrt{3}}}-1}{e^{\frac{\pi}{\sqrt{3}}}+1} - \frac{C(Y)\,Y}{4e^{\frac{\pi}{\sqrt{3}}}\left(e^{\frac{\pi}{\sqrt{3}}}+1\right)}\delta^2 + O(\delta^3),$$

where $C(Y)$ is given in expression (15).

Therefore, the existence of the functions τ_C^S and a_S, as well as the analyticity of functions $a_S(Y,\varepsilon)$ and $\sqrt{\varepsilon}\,\tau_C^S(Y,\varepsilon)$ as functions of $\sqrt{\varepsilon}$ and the validity of expressions (13) and (14), are guaranteed by undoing the change of variable (20). Here, functions $\tau_C^S(Y,\varepsilon) = \eta_S(Y,\sqrt{\varepsilon})/\sqrt{\varepsilon}$ and $a_S(Y,\varepsilon) = \sqrt{\varepsilon}\,A_S(Y,\sqrt{\varepsilon})$ are defined in $(Y_0-\mu, Y_0+\mu)\times\left(0,\mu^2\right)$.

Now, we will turn to proving that the last inequality of (17) is satisfied by assuring that $x_C'(\tau;a_S,\varepsilon) < 0$ for $\tau \in (0,\tau_C^S)$. On the contrary let us assume that there exists $t_1 \in (0,\tau_C^S)$ such that $x_C'(t_1;a_S,\varepsilon) = 0$. Therefore the point $(x_C(t_1;a_S,\varepsilon), y_C(t_1;a_S,\varepsilon))$ belongs to the x-nullcline with $x_C(t_1;a_S,\varepsilon) < -\sqrt{\varepsilon}$. We conclude that $(-\sqrt{\varepsilon}, y_C(\tau_C^S;a_S,\varepsilon)) = \mathbf{q}_0^L + Y_0\varepsilon^{-\frac{3}{2}}(0,1)^T$ with $Y_0 > \widetilde{Y}_0$. Notice that $\widetilde{Y}_0 = \widetilde{Y}_0^*$ since $a = a_S$, and then $Y_0 > \widetilde{Y}_0^*$ in contradiction with the hypotheses.

4.2 Proof of Theorem 3.3

Theorem 3.3 is devoted to the existence and stability of the curve of limit cycles which starts at the Hopf-like bifurcation. In this result we also distinguish between the different oscillatory regimes taking place along the curve, those are the Hopf like cycles, the canard cycles and the relaxation oscillations. All these oscillatory regimes are characterised according to whether the limit cycles evolve close to the repelling slow manifold or not. In particular, the canard regime is formed by all the cycles that flow close to the repelling slow manifold, and therefore that intersect the separation plane $\{x = -\sqrt{\varepsilon}\}$ exponentially close to $\mathbf{q}_0^L$. Moreover, the canard regime is inserted between the Hopf and the relaxation regimes. Nevertheless, as far as we are concerned, the transitions between these regimens are not precisely defined in the literature. By analyzing the strong divergence in the neighbourhood of the unstable slow manifold, in the next result we suggest two cycles of the one-parameter family to act as boundaries of the previous oscillatory regimes.

Lemma 4.1 *For $\varepsilon_0 > 0$ sufficiently small, set $\varepsilon < \varepsilon_0$, $a < \sqrt{\varepsilon}$ and let Γ_{x_0} be a limit cycle of system* (1) *having width $x_0 \in (-\infty, a)$. Consider the values of x_r and x_s given in* (16)*. It holds that:*

a) If $x_0 \in (x_s, a)$ then Γ_{x_0} is under Hopf regime.

b) If $x_0 \in (x_r, x_s)$ then Γ_{x_0} is under canard regime.

c) If $x_0 \in (-\infty, x_r)$ then Γ_{x_0} is under relaxation regime.

Proof: The proof of the result is obtained through the analysis of the divergence in a neighbourhood of the repelling slow manifold, S_ε^r, contained in the zone σ_L, see Figure 4. To this end, we consider the transition map from points on the switching line $\{x = -\sqrt{\varepsilon}\}$ to itself, but also the transition map to the switching line $\{x = -1\}$. Since $\mathbf{p}_L$ and $\mathbf{p}_{LL}$ are contact points of the flow with the switching lines, the domain and the ranges of these transition maps can be parametrized as follows, $\mathbf{p}_L - u\dot{\mathbf{p}}_L$ with $u > 0$ and $\mathbf{p}_L + v\dot{\mathbf{p}}_L$ or $\mathbf{p}_{LL} - v\dot{\mathbf{p}}_{LL}$ with $v > 0$, respectively, where $\dot{\mathbf{p}}_L$ and $\dot{\mathbf{p}}_{LL}$ stand for the vector field evaluated at points $\mathbf{p}_L$ and $\mathbf{p}_{LL}$ respectively, see Figure 5.

Let $\varphi(t)$ be a solution of system (1) such that $\varphi(t) \subset \sigma_L$ for $t \in (0,t_0)$ and $t_0 > 0$. By using the Krylov base $\{\mathbf{p}_L, \dot{\mathbf{p}}_L\}$, the solution can be parametrized by $\varphi(t) = u_1(t)\mathbf{p}_L + u_2(t)\dot{\mathbf{p}}_L$. Following Theorem 5 in [26], function $H_L(u_1,u_2) = |u_1+\lambda_L^s u_2|^{\lambda_L^q}|u_1+\lambda_L^q u_2|^{-\lambda_L^s}$ is constant over the coordinates $(u_1(t),u_2(t))$ with $t \in (0,t_0)$, and it is called a first integral for system (1) related to the Krylov base $\{\mathbf{p}_L, \dot{\mathbf{p}}_L\}$. Therefore, the transition map from points on the switching line $\{x = -\sqrt{\varepsilon}\}$ to itself, i. e., from points $\mathbf{p}_L - u\dot{\mathbf{p}}_L$ to points $\mathbf{p}_L + v\dot{\mathbf{p}}_L$, is given by $H_L(1,-u) = H_L(1,v)$, that is

$$\frac{|1-u\lambda_L^s|^{\lambda_L^q}}{|1-u\lambda_L^q|^{\lambda_L^s}} = \frac{|1+v\lambda_L^s|^{\lambda_L^q}}{|1+v\lambda_L^q|^{\lambda_L^s}}, \tag{23}$$

for $u \in [0,u_t)$, where u_t is the coordinate of the initial condition $\mathbf{p}_L - u_t\dot{\mathbf{p}}_L$ of the orbit passing through $\mathbf{p}_{LL}$. Consequently, u_t limits the domain of the transition map from the straight line $\{x = -\sqrt{\varepsilon}\}$ to itself, and it is at the same time the beginning of the transition map between the two switching lines, see Figure 5.

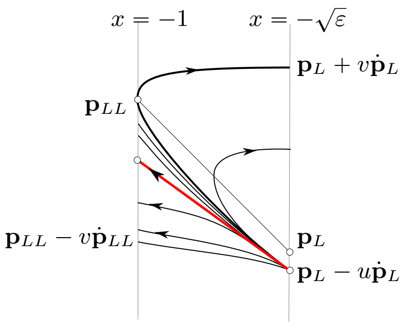

Figure 5: **Transition maps in σ_L.** Representation of the transition maps from $\{x = -\sqrt{\varepsilon}\}$ to itself and to $\{x = -1\}$ in terms of the Krylov bases $\{\mathbf{p}_L, \dot{\mathbf{p}}_L\}$ and $\{\mathbf{p}_{LL}, \dot{\mathbf{p}}_{LL}\}$.

On the other hand, since $\mathbf{p}_{LL} - \mathbf{e}_L = r(\mathbf{p}_L - \mathbf{e}_L)$ and $\dot{\mathbf{p}}_{LL} = r\dot{\mathbf{p}}_L$ with

$$r = \frac{\|\mathbf{p}_{LL} - \mathbf{e}_{LL}\|}{\|\mathbf{p}_L - \mathbf{e}_L\|} = \frac{1+a}{\sqrt{\varepsilon}+a},$$

it follows that the transition map from points $\mathbf{p}_L - u\dot{\mathbf{p}}_L$ to points $\mathbf{p}_{LL} - v\dot{\mathbf{p}}_{LL}$ is given by $H_L(1, -u) = H_L(r, -rv)$, that is

$$\frac{|1 - u\lambda_L^s|^{\lambda_L^q}}{|1 - u\lambda_L^q|^{\lambda_L^s}} = r^{\lambda_L^q - \lambda_L^s} \frac{|1 - v\lambda_L^s|^{\lambda_L^q}}{|1 - v\lambda_L^q|^{\lambda_L^s}}, \tag{24}$$

with $u \in [u_t, +\infty)$. The value of u_t can be computed from (24) since $v(u_t) = 0$, that is

$$u_t = \frac{1}{\lambda_L^q} - \frac{1}{\lambda_L^q} e^{\frac{1}{2\lambda_L^s}\ln(\varepsilon)} \in \left(1, \frac{1}{\lambda_L^q}\right).$$

Therefore, expressions (23)-(24) define the transition map $v(u)$ implicitely given as

$$F(u) = \begin{cases} F(-v), & u \in [0, u_t), \\ r^{\lambda_L^q - \lambda_L^s} F(-v), & u \in [u_t, +\infty], \end{cases} \tag{25}$$

where $F(x)$ is defined by

$$F(x) = \frac{|1 - x\lambda_L^s|^{\lambda_L^q}}{|1 - x\lambda_L^q|^{\lambda_L^s}} = \begin{cases} \dfrac{(1 - x\lambda_L^s)^{\lambda_L^q}}{(1 - x\lambda_L^q)^{\lambda_L^s}}, & \text{if } x < 1/\lambda_L^q, \\ \dfrac{(1 - x\lambda_L^s)^{\lambda_L^q}}{(x\lambda_L^q - 1)^{\lambda_L^s}}, & \text{if } 1/\lambda_L^q < x < 1/\lambda_L^s, \\ \dfrac{(x\lambda_L^s - 1)^{\lambda_L^q}}{(x\lambda_L^q - 1)^{\lambda_L^s}}, & \text{if } x > 1/\lambda_L^s. \end{cases} \tag{26}$$

In Figure 6 it is depicted the graphs of the functions $F(x)$ and $r^{\lambda_L^q - \lambda_L^s} F(x)$ together with a representation of the transition map $v(u)$.

From (7) and (8) it follows that $\mathbf{q}_0^L = \mathbf{p}_L - \frac{1}{\lambda_L^q}\dot{\mathbf{p}}_L$, thus the coordinate $u = \frac{1}{\lambda_L^q}$ corresponds to the repelling slow manifold S_ε^r. Hence, the canard orbits are those with coordinate u exponentially close to it. Let $u_s(\varepsilon) < \frac{1}{\lambda_L^q}$ be such that $F(u_s(\varepsilon)) = 1 + \frac{1}{|\ln(\varepsilon)|}$. According to expression (41) it follows that

$$u_s(\varepsilon) = \frac{1}{\lambda_L^q} - \frac{1}{\lambda_L^q} e^{-\frac{1}{\varepsilon|\ln(\varepsilon)|}},$$

which is a canard orbit, as well as every u such that $u_s(\varepsilon) \leqslant u \leqslant \frac{1}{\lambda_L^q}$. Therefore, we suggest $u_s(\varepsilon)$ to be the lower boundary of the canard regimen.

Let us now compute x_s, that is, the first coordinate of the intersection of the orbit passing through $\mathbf{p}_L - u_s(\varepsilon)\dot{\mathbf{p}}_L$ with the $x-$nullcline. The transition map from points in $\{x = -\sqrt{\varepsilon}\}$ into points in the $x-$nullcline in zone σ_L is given by,

$$H_L(1, -u_s(\varepsilon)) = H_L(\gamma, 0). \tag{27}$$

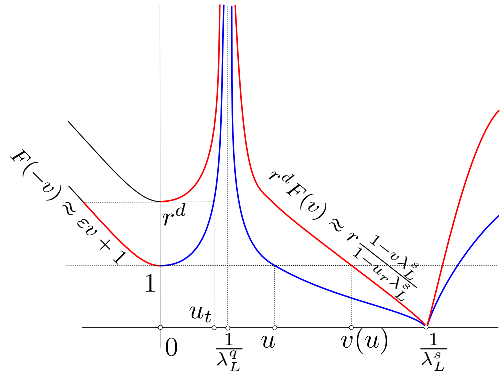

Figure 6: **Representation of the transition map** $v(u)$ throught the graphs of the functions $F(x)$ and $r^{\lambda_L^q-\lambda_L^s}F(x) = r^dF(x)$, with $d = \lambda_L^q - \lambda_L^s$. Note that $v(u) = u$ at $u = \frac{1}{\lambda_L^q}$ and $u = \frac{1}{\lambda_L^s}$.

Moreover, $H_L(1, -u_s(\varepsilon)) = F(u_s(\varepsilon))$ and by construction $F(u_s(\varepsilon)) = 1 + \frac{1}{|\ln(\varepsilon)|}$. Also, $H_L(\gamma, 0) = \gamma^{\lambda_L^q-\lambda_L^s}$ which can be approximated at first order by γ. Taking this into account, from (27) we find that $\gamma \approx 1 + \frac{1}{|\ln(\varepsilon)|}$. Thus, x_s can be computed as the first coordinate of the point $\mathbf{e}_L + \gamma(\mathbf{p}_L - \mathbf{e}_L)$, from which we obtain expression (16).

On the other hand, consider $\frac{1}{\lambda_L^q} < u_r(\varepsilon) < \frac{1}{\lambda_L^s}$ such that $F(u_r) = 1 + \frac{1}{|\ln(\varepsilon)|}$. According to expression (41) it follows that

$$u_r(\varepsilon) = \frac{1}{\lambda_L^q} + \frac{1}{\lambda_L^q} e^{-\frac{1}{\varepsilon|\ln(\varepsilon)|}},$$

which is a canard orbit, as well as every u such that $\frac{1}{\lambda_L^q} \leqslant u \leqslant u_r(\varepsilon)$. Therefore, we suggest $u_r(\varepsilon)$ to be the upper boundary of the canard regimen. Let $v_r = v(u_r)$, from expression (25) and by using that $F(u_r) = 1 + \frac{1}{|\ln(\varepsilon)|}$ and

$$r^{\lambda_L^q-\lambda_L^s} F(-v) = r^{\lambda_L^q-\lambda_L^s} \frac{1 - v\lambda_L^s}{1 - u_r\lambda_L^s} \approx r \frac{1 - v\lambda_L^s}{1 - u_r\lambda_L^s},$$

we conclude that $v_r(\varepsilon) = \frac{1}{\lambda_L^s}\left(1 - \sqrt{\varepsilon}\left(1 + \frac{1}{|\ln(\varepsilon)|}\right)\right)$.

Let us finally compute the first coordinate, x_r, of the intersection point with the $x-$nullcline, of the orbit through $\mathbf{p}_L - u_r(\varepsilon)\dot{\mathbf{p}}_L$. From definition, orbit passing through the point $\mathbf{p}_L - u_r(\varepsilon)\dot{\mathbf{p}}_L$ also passes through the point $\mathbf{p}_v = \mathbf{p}_{LL} - v_r(\varepsilon)\dot{\mathbf{p}}_{LL}$, and $\mathbf{p}_v$ can also be written as $\mathbf{p}_v = \mathbf{p}_{LL} - y_r\mathbf{e}_2$, where $y_r = \lambda_L^q - \lambda_L^q\sqrt{\varepsilon}(1 + \frac{1}{|\ln(\varepsilon)|})$. Thus, from the first expression in (9) with $d = y_r$, expression (16) follows.

□

Now we deal with the proof of the Theorem 3.3. First, we prove the existence of the family of cycles, and second we study the stability of these cycles.

Let $\bar{\mathbf{p}}_0 = (-\sqrt{\varepsilon}, y)$ be the intersection point of the orbit through $(x_0, f(x_0))$ with the separation line $\{x = -\sqrt{\varepsilon}\}$, and consider $\mathbf{p}_0 = \mathbf{q}_0^L + Y_0\varepsilon^{\frac{3}{2}}(0,1)^T$ exponentially close to $\bar{\mathbf{p}}_0$. Since $x_0 < x_s$ it follows that $Y_0 < Y_s < \widetilde{Y}_0^*$, where $\widetilde{Y}_0^*$ is given in (12) and

$$Y_s = \frac{2e^{\frac{\pi}{\sqrt{3}}}}{e^{\frac{\pi}{\sqrt{3}}} + 1} e^{-\frac{1}{\varepsilon|\ln(\varepsilon)|}}$$

corresponds with the orbit through $(x_s, f(x_s))$. By integrating forward, at some point the orbit will cross from the central to the right zone in $O(\varepsilon)$ time, and will reach a neighborhood of S_ε^a. After that, as the manifold S_ε^a is attracting, the orbit targets to the central zone, while the distance to S_ε^a is contracting with contraction rate $O(\exp(-c/\varepsilon))$, where c is a positive constant depending on y, for a time interval of order $O(1)$. Thus, the orbit arrives to the central zone in a point $\bar{\mathbf{p}}_1$, which is exponentially close to the intersection between the invariant manifold S_ε^a and the separation line $\{x = \sqrt{\varepsilon}\}$, that is, $\mathbf{q}_1^R$ given in expression (6).

Consider now the connection between $\bar{\mathbf{p}}_1$ and $\bar{\mathbf{p}}_0$. Following the proof of Theorem 3.2, this connection can be obtained as the solutions of a system of two equation, namely $\bar{F}_1(\tau, a, \varepsilon, Y_0) = 0$

and $\bar{F}_2(\tau, a, \varepsilon, Y_0) = 0$. Moreover, since $\bar{\mathbf{p}}_1$ and $\bar{\mathbf{p}}_0$ are exponentially close to $\mathbf{q}_1^R$ and $\mathbf{p}_0$ respectively, the change of variables (20) transforms the previous system into

$$\begin{pmatrix} G_1(\eta, A, \delta) \\ G_2(\eta, A, \delta, Y_0) \end{pmatrix} + \boldsymbol{\xi}(y, \eta, A, \delta, Y_0) = \begin{pmatrix} 0 \\ 0 \end{pmatrix}, \tag{28}$$

where G_1 and G_2 are the functions in (21)-(22) and being $\boldsymbol{\xi}(y, \eta, A, \delta, Y_0)$ and their derivatives are $O(\exp(-c/\delta^2))$ small, where c is a positive constant depending on y. Thus, we can apply the Implicit Function Theorem for $\mathcal{C}^\infty$ functions to the set of equations (28) which proves the existence of two $\mathcal{C}^\infty$ functions A_N and η_N defined in a neigbourhood of Y_0 and $\delta = 0$ and such that $(y, \eta_N(Y, \delta), A_N(Y, \delta), \delta, Y)$ is a solution of systems (28). Moreover, functions A_N and η_N are exponentially close to functions A_S and τ_C^S, respectively, which are obtained in Theorem 3.2.

Finally, since Y_0 depends on x_0 and $\delta = \sqrt{\varepsilon}$ we consider A_N and η_N as defined in $(x_0 - \mu, x_0 + \mu) \times (-\sqrt{\mu}, \sqrt{\mu})$. This concludes the proof of the existence of a periodic orbit Γ_{x_0} passing through $(x_0, f(x_0))$ when $x_0 \in (-\infty, x_s)$.

We study now the stability of such limit cycle Γ_{x_0}. To this end, let us consider the derivative with respect to the width x of the Poincaré map introduced in Definition 2.1. It corresponds to the exponential of the integral of the divergence along the limit cycle, see [7]. In the particular case of PWL systems, the integral of the divergence can be explicitly computed as the sum of the product of the trace and the time of flight, as they are introduced in Definition 2.2, of the limit cycle in each region of linearity, see [21],

$$\frac{\partial \Pi}{\partial x}(x_0, a_N(x_0, \varepsilon), \varepsilon) = e^{t_L \tau_L + t_{LL}\tau_{LL} + t_R \tau_R + t_c \tau_C} = e^{\tau_L - \tau_R + \sqrt{\varepsilon}\tau_C}, \tag{29}$$

where we have taken into account the values of the traces in each zone, see (3). Therefore, the stability of Γ_{x_0} depends on the sign of $\tau_L - \tau_R + \sqrt{\varepsilon}\tau_C$.

The time τ_C that the orbit takes in zone σ_C is divided into two parts, one below and another above the $x-$nullcline. Thus, we can write that, $\tau_C = \tau_{Cd} + \tau_{Cu}$, where $\tau_{Cd} = \tau_C^S(Y, \varepsilon) = \frac{2\pi}{\sqrt{3}\sqrt{\varepsilon}} + O(\varepsilon)$, see Theorem 3.2, and $\tau_{Cu} = O(\varepsilon)$.

In the following, we calculate the sign of $\tau_L - \tau_R + \sqrt{\varepsilon}\tau_C$ depending on whether Γ_{x_0} is a headless canard, a canard with head or a relaxation oscillation.

Suppose the cycle is a headless canard. In such a case, the cycle intersects the switching line $\{x = -\sqrt{\varepsilon}\}$ above the $x-$nullcline at a point whose second coordinate is denoted by h. In Lemma A.1 we present the times of flight of the cycle as a function of h and so

$$\tau_L - \tau_R = \frac{1}{\lambda_L^s} \ln \left(\frac{((\lambda_L^q - \sqrt{\varepsilon})(\sqrt{\varepsilon} + a_N) + h)\,(\lambda_R^q - \lambda_R^s)(\sqrt{\varepsilon} - a_N)}{((\lambda_R^q - \sqrt{\varepsilon})(\sqrt{\varepsilon} - a_N) - h)\,(\lambda_L^q - \lambda_L^s)(\sqrt{\varepsilon} + a_N)} \right),$$

where $\lambda_L^s = -\lambda_R^s$, $\lambda_L^q = -\lambda_R^q$ and $a_N = a_0\sqrt{\varepsilon} + O(\varepsilon)$ with $a_0 = \frac{e^{\frac{\pi}{\sqrt{3}}} - 1}{e^{\frac{\pi}{\sqrt{3}}} + 1}$, see (13). Hence,

$$\begin{aligned} \tau_L - \tau_R &= \frac{1}{\lambda_L^s} \ln \left(-\frac{((\lambda_L^q - \sqrt{\varepsilon})(1 + a_0 + O(\sqrt{\varepsilon}))\sqrt{\varepsilon} + h)\,(1 - a_0 + O(\sqrt{\varepsilon}))}{((\lambda_R^q - \sqrt{\varepsilon})(1 - a_0 + O(\sqrt{\varepsilon}))\sqrt{\varepsilon} - h)\,(1 + a_0 + O(\sqrt{\varepsilon}))} \right), \\ &= \frac{1}{\lambda_L^s} \ln \left(\frac{1 - a_0}{1 + a_0} + O(\sqrt{\varepsilon}) \right) = -\frac{C^2}{\varepsilon} + O(\varepsilon^{-1/2}). \end{aligned}$$

Therefore, for ε small enough $\tau_L - \tau_R + \sqrt{\varepsilon}\tau_C < 0$ which implies that $\frac{\partial \Pi}{\partial y}(x_0, \boldsymbol{\eta}) < 1$ and so headless canard cycles are all stable limit cycles.

Assume now that Γ_{x_0} is a canard cycle with head or a relaxation oscillation. Then Γ_{x_0} intersects the switching line $\{x = -1\}$ into two points, $\mathbf{p}_{LL}^+$ and $\mathbf{p}_{LL}^-$, one above and the other below $\mathbf{p}_{LL}$ and equidistant to it, since the trace $t_{LL} = 0$. Let h_+ and h_- be the second coordinates of $\mathbf{p}_{LL}^+$ and $\mathbf{p}_{LL}^-$, respectively.

In the case Γ_{x_0} is a canard cycle with head, we can write that $\tau_L = \tau_{Ld} + \tau_{Lu}$, where τ_{Lu} corresponds with the time of the transition of the cycle in σ_L above the nullcline. Since the dynamics at this part is fast, hence the contribution of τ_{Lu} is neglibible with respect to τ_{Ld} and will not be taken into account in following computations. From Lemma A.1, taking $h = h_-$ in the computation of $\tau_{Ld}(h)$ and $h = h_+$ in the computation of $\tau_R(h)$, it follows that

$$\tau_{Ld} - \tau_R = \frac{1}{\lambda_L^s} \ln \left(\frac{((\lambda_L^q - \sqrt{\varepsilon})(\sqrt{\varepsilon} + a_N) + \lambda_L^s(\sqrt{\varepsilon} - 1) + h_-)\,(\lambda_R^q - \lambda_R^s)(\sqrt{\varepsilon} - a_N)}{((\lambda_R^q - \sqrt{\varepsilon})(\sqrt{\varepsilon} - a_N) - h_+)\,(\lambda_L^q - \lambda_L^s)(\sqrt{\varepsilon} + a_N)} \right),$$

where $\lambda_L^s = -\lambda_R^s$, $\lambda_L^q = -\lambda_R^q$ and $a_N = a_0\sqrt{\varepsilon} + O(\varepsilon)$. Hence,

$$\tau_{Ld} - \tau_R = \frac{1}{\lambda_L^s} \ln\left(-\frac{((\lambda_L^q - \sqrt{\varepsilon})(1 + a_0 + O(\sqrt{\varepsilon}))\sqrt{\varepsilon} + \lambda_L^s(\sqrt{\varepsilon} - 1) + h_-)(1 - a_0 + O(\sqrt{\varepsilon}))}{((\lambda_R^q - \sqrt{\varepsilon})(1 - a_0 + O(\sqrt{\varepsilon}))\sqrt{\varepsilon} - h_+)(1 + a_0 + O(\sqrt{\varepsilon}))}\right)$$
$$= \frac{1}{\lambda_L^s} \ln\left(\frac{h_-}{h_+}\frac{1 - a_0}{1 + a_0} + O(\sqrt{\varepsilon})\right) = -\frac{C^2}{\varepsilon} + O(\varepsilon^{-1/2}),$$

with $h_- < h_+$. Therefore, $\tau_L - \tau_R + \sqrt{\varepsilon}\tau_C < 0$ and canard cycles with head are also stable limit cycles.

Assuming now that Γ_{x_0} be a relaxation oscillation, then the piece of the orbit in σ_L under the x-nullcline flows along the fast dynamics so in this case τ_{Ld} is negligible with respect to τ_R which is order -1 in ε. Therefore $\tau_L - \tau_R + \sqrt{\varepsilon}\tau_C < 0$ and the relaxation oscillations are stable limit cycles. This ends the proof of Theorema 3.3.

4.3 Proof of Theorem 3.4

We begin by proving statement (a) and after that we proceed to prove statement (b).

For ε small enough, let us consider the period function $T(x, \varepsilon)$ introduced in Definition 2.2 with $a = a_N(x, \varepsilon) = a_S(0, \varepsilon)$ if $x \in (x_r, x_s)$, or $a = a_S(Y(h_2(x)), \varepsilon)$ otherwise, and given by

$$T(x, \varepsilon) = \begin{cases} \tau_L(h_1(x)) + \tau_R(h_1(x)) + \tau_C & x \in [-1, x_s), \\ \tau_{Ld}(h_2(x)) + \tau_{LL}(h_2(x)) + \tau_R(2p_2 - h_2(x)) + \tau_C & x \in (x_r, -1), \\ \tau_{LL}(h_2(x)) + \tau_R(2p_2 - h_2(x)) + \tau_C^S(Y(h_2(x)), \varepsilon) & x < x_r, \end{cases} \tag{30}$$

where $p_2 = 1 + \varepsilon + \sqrt{\varepsilon}(a - 1)$ is the second component of the tangent point $\mathbf{p}_{LL}$ given in (8), functions $\tau_L(h), \tau_{Ld}(h)$, $\tau_{LL}(h)$ and $\tau_R(h)$ are the time of flight introduced in Definition 2.2 and computed in Lemma A.1, and $\tau_C = \tau_C^S(0, \varepsilon)$ where $\tau_C^S(Y, \varepsilon)$ is given in (14). Moreover, $h_1(x)$ and $h_2(x)$ provide the second coordinate of the intersection points, if any, of the cycle Γ_x with the switching lines $\{x = -\sqrt{\varepsilon}\}$ and $\{x = -1\}$, respectively. In particular, if $x \in (-1, x_s)$, then $h_1(x)$ is the second coordinate of the intersection point of Γ_x with $\{x = -\sqrt{\varepsilon}\}$ which is above of the tangent point $\mathbf{p}_L$. If $x \in (-\infty, -1)$, then $h_2(x)$ is the second coordinate of the intersection point of Γ_x with $\{x = -1\}$ which is below $\mathbf{p}_{LL}$. We note that when ε is small enough and $x < x_r$, then $h_2(x)$ also provides a good approximation for the second coordinate of the intersection point of the orbit Γ_x with $\{x = -\sqrt{\varepsilon}\}$ which is below $\mathbf{p}_L$, see Figure 4. Therefore, function $Y(h_2(x))$ and its derivative $\frac{dY}{dh}$ can be obtained from equation $h_2(x) = (\sqrt{\varepsilon} - \lambda_L^s)(\sqrt{\varepsilon} + a_S(Y, \varepsilon)) + Y\varepsilon^{\frac{3}{2}}$, corresponding with the second coordinate of the equation (10). Hence, $\frac{dY}{dh} = \left(\varepsilon^{\frac{3}{2}} + (\sqrt{\varepsilon} - \lambda_L^s)\frac{\partial a_S}{\partial Y}\right)^{-1}$, where $\frac{\partial a_S}{\partial Y} = \varepsilon^{\frac{3}{2}}\frac{4e^{\frac{\pi}{\sqrt{3}}} - 2(1 + e^{\frac{\pi}{\sqrt{3}}})Y}{4e^{\frac{\pi}{\sqrt{3}}}(1 + e^{\frac{\pi}{\sqrt{3}}})} + O(\varepsilon^2) > 0$ can be computed from (13), and therefore

$$\frac{dY}{dh} = \varepsilon^{-\frac{3}{2}} + O(\varepsilon^{-1}). \tag{31}$$

Set

$$h(x) = \begin{cases} h_1(x), & x \in [-1, x_s), \\ h_2(x), & x \in (-\infty, -1). \end{cases}$$

It is easy to see that $\frac{dh}{dx} > 0$ in $(-\infty, -1)$ and $\frac{dh}{dx} < 0$ in $(-1, x_s)$.

From Lemma A.1 and since $\lambda_L^q = -\lambda_R^q$, the derivative of the period function given in (30) for $x \in [-1, x_s)$ can be straightforward computed as

$$\begin{aligned} \frac{\partial T}{\partial x} &= (\tau_L'(h) + \tau_R'(h))\frac{dh}{dx} \\ &= \frac{1}{\lambda_L^s}\frac{dh}{dx}\left(\frac{1}{(\lambda_L^q - \sqrt{\varepsilon})(\sqrt{\varepsilon} + \tilde{a}) + h} - \frac{1}{(\lambda_R^q - \sqrt{\varepsilon})(\sqrt{\varepsilon} - \tilde{a}) - h}\right) \\ &= \frac{1}{\lambda_L^s}\frac{dh}{dx}\left(\frac{1}{(\lambda_L^q - \sqrt{\varepsilon})(\sqrt{\varepsilon} + \tilde{a}) + h} + \frac{1}{(\lambda_L^q + \sqrt{\varepsilon})(\sqrt{\varepsilon} - \tilde{a}) + h}\right) < 0, \end{aligned}$$

where $\tilde{a} = a_S(\varepsilon, 0)$, see (13).

On the other hand, for $x \in (x_r, -1)$ the derivative of the period function is given as,

$$\frac{\partial T}{\partial x} = (\tau_{Ld}'(h) + \tau_{LL}'(h) - \tau_R'(2p_2 - h))\frac{dh}{dx}. \tag{32}$$

From Lemma A.1,

$$\begin{aligned}\tau'_{Ld}(h)+\tau'_{LL}(h)-\tau'_R(2p_2-h)=&\frac{1}{\lambda_L^s}\frac{1}{(\lambda_L^q-\sqrt{\varepsilon})(\sqrt{\varepsilon}+\tilde{a})+\lambda_L^s(\sqrt{\varepsilon}-1)+h}\\&-\frac{2(1+\tilde{a})}{\varepsilon(1+\tilde{a})^2+(1-h+\sqrt{\varepsilon}(\tilde{a}-1)+\varepsilon)^2}\\&+\frac{1}{\lambda_L^s}\frac{1}{(\lambda_R^q-\sqrt{\varepsilon})(\sqrt{\varepsilon}-\tilde{a})-2(1+\sqrt{\varepsilon}(\tilde{a}-1)+\varepsilon)+h}\end{aligned}$$

and taking into account the value of $\tilde{a}=a_S(\varepsilon,0)$, it follows that expression (32) writes as

$$\frac{\partial T}{\partial x}=\left(\frac{1}{\varepsilon}\left(\frac{1}{h}+\frac{1}{h-2}\right)-\frac{2}{(1-h)^2}+O(\sqrt{\varepsilon})\right)\frac{dh}{dx}. \tag{33}$$

Since $dh/dx>0$ in $(x_r,-1)$ the function $\frac{\partial T}{\partial x}$ has an unique zero

$$h^*=1-\varepsilon^{\frac{1}{3}}+\frac{1}{3}\varepsilon-\frac{1}{9}\varepsilon^{\frac{5}{3}}+O(\varepsilon^3), \tag{34}$$

which is positive at $(0,h^*)$, and negative in (h^*,p_2). Consequently, T has a local maximum at h^*, corresponding with a canard cycle with width $x_P\in(x_r,-1)$.

Finally, for $x\in(-\infty,x_r)$ the derivative of the period function is given as,

$$\frac{\partial T}{\partial x}=\left(\tau'_{LL}(h)-\tau'_R(2p_2-h)+\frac{\partial\tau_C^S}{\partial Y}\frac{dY}{dh}\right)\frac{dh}{dx}. \tag{35}$$

From Theorem 3.2 and expression (31), we get,

$$\frac{\partial\tau_C^S}{\partial Y}\frac{dY}{dh}=\frac{1+e^{\frac{\pi}{\sqrt{3}}}}{2e^{\frac{\pi}{\sqrt{3}}}}\varepsilon^{-\frac{3}{2}}+O(\varepsilon^{-1}). \tag{36}$$

On the other side, from Lemma A.1 it follows that

$$\tau'_{LL}(h)-\tau'_R(2p_2-h)=-\frac{2(1+a)}{(1-h)^2}+\frac{1}{\varepsilon(h-2+a)},$$

where we note that a is not necessarily of order $\sqrt{\varepsilon}$ since we are considering $x\in(-\infty,x_r)$. Therefore, taking into account (36), it follows that the expression (35) writes as

$$\frac{\partial T}{\partial x}=\left(\frac{1+e^{\frac{\pi}{\sqrt{3}}}}{2e^{\frac{\pi}{\sqrt{3}}}}\varepsilon^{-\frac{3}{2}}+O(\varepsilon^{-1})\right)\frac{dh}{dx},$$

and then $\partial T/\partial x>0$ in $(-\infty,x_r)$ since $dh/dx>0$ in that interval. Thus, this conclude the proof of statement (a).

Now, let us proceed to the proof of statement (b).

Taking into account that $p_2=1+\varepsilon+\sqrt{\varepsilon}(\tilde{a}-1)$ is the second coordinate of the point $\mathbf{p}_{LL}$, the change of coordinates from the height h_2 to the width x is given by the expression (9) with $d=p_2-h$ and $a=\tilde{a}$, i.e.,

$$x=-\frac{\sqrt{(p_2-h)^2+(\tilde{a}+1)^2\varepsilon}-\tilde{a}\sqrt{\varepsilon}}{\sqrt{\varepsilon}}.$$

Using this change of variables, we conclude that the width x_P of the canard cycle with maximum period can be computed as

$$x_P=-\frac{\sqrt{(p_2-h^*)^2+(\tilde{a}+1)^2\varepsilon}-\tilde{a}\sqrt{\varepsilon}}{\sqrt{\varepsilon}}=-\varepsilon^{-\frac{1}{6}}+O(\varepsilon^{\frac{1}{2}}).$$

Since $x_r=-\varepsilon^{-\frac{1}{2}}+O(\varepsilon^0)$, from (16), this maximum is clearly located in the interval $(x_r,-1)$. Moreover, the value of the period (30) at x_P can be computed as

$$\begin{aligned}T(x_P,\varepsilon)&=\tau_{Ld}(h^*)+\tau_{LL}(h^*)+\tau_R(2p-h^*)+\tau_C\\&=\frac{1}{\varepsilon}\ln\left(\frac{h^*}{\sqrt{\varepsilon}+\tilde{a}}\right)+\frac{2}{\sqrt{\varepsilon}}\arctan\left(\frac{1-h^*}{\sqrt{\varepsilon}}\right)-\frac{1}{\varepsilon}\ln\left(\frac{h^*-2p_2}{\tilde{a}-\sqrt{\varepsilon}}\right)\\&=\frac{1}{\varepsilon}\ln\left(\frac{h^*(2-h^*)}{\varepsilon-\tilde{a}^2}\right)+\frac{2}{\sqrt{\varepsilon}}\arctan\left(\frac{1-h^*}{\sqrt{\varepsilon}}\right).\end{aligned}$$

Finally, substituting in the previous expression the value of h^* given in (34) and the value of $\widetilde{a} = a_S(0, \varepsilon)$, we obtain the maximum of the period,

$$T(x_P(\varepsilon), \varepsilon) = \frac{1}{\varepsilon} \ln \left(\frac{C_0(1 - \varepsilon^{\frac{2}{3}})}{\varepsilon} \right) + O(\varepsilon^{-\frac{1}{2}}),$$

where,

$$C_0 = \frac{(1 + e^{\frac{\pi}{\sqrt{3}}})^2}{4e^{\frac{\pi}{\sqrt{3}}}}.$$

4.4 Proof of Theorem 3.5

From the expression of x_r in (16) and the expression of $x_P(\varepsilon)$ appearing in Theorem 3.4, and assuming ε small enough, it follows that $x_r < x_P(\varepsilon) < -1$. Since $\widetilde{x}(\varepsilon)$ is the width of the canard cycle through the point $\mathbf{q}_1^L$ and $\mathbf{q}_1^L = \mathbf{p}_{LL} - (1 + \widetilde{a})\lambda_L^s \mathbf{e}_2$, from (9) it follows that

$$\widetilde{x}(\varepsilon) = -1 - \frac{1}{2}\varepsilon + O(\varepsilon^{\frac{3}{2}}).$$

Therefore,

$$x_r < x_P(\varepsilon) < \widetilde{x}(\varepsilon) < -1.$$

On the other hand, the absolute value of the width x_M of the maximal canard cycle taking place when both branches of the slow manifold connect is smaller than $|\widetilde{x}(\varepsilon)|$, and the theorem follows.

5 Conclusions

In this paper we have further described the canard regime as a part of the canard explosion in a PWL slow-fast system exhibiting a flat critical manifold. In particular, we have suggested two canard cycles acting as a boundaries of the canard regime, see (16), which define the birth and the maturation of the canards. Even when the canard regime occurs in an exponentially small interval of the parameter, the flatness of the critical manifold allows an interval of the width of the canard cycles, (x_r, x_s), to become non-bounded as ε tends to zero. Thus, regarding to the width of the cycles, canards appear further apart from one another, allowing for a deep analysis of the transitional region going from the headless canard cycles to the canard cycles with head. Therefore, we have also located the transitory canard cycle, the maximal canard cycle, the canard cycle flowing along the slow repelling manifold, which defines the quasi-threshold, and the maximum period canard cycle. In Theorem 3.5 it is proved that these canard cycles are all different dynamical objects. Moreover, it can be concluded that the width of the three first cycles converge to -1 as ε tends to zero, corresponding with the width of the transitory canard; whereas the width of the maximun period canard cycle converges to $-\infty$.

Apart from the results obtained on the different canard cycles in the transient regime, we highlight the study carried out on the period function $T(x, \varepsilon)$, whose unimodal character has been proved, and an estimate for the maximum period has been obtained. This type of quantitative estimation are difficult to derive in the smooth context and can be highly appreciated in applications, see [30] and references therein.

The analysis developed along the manuscript has been carried out by taking advantage not only of the PWL context, but also of the existence of the flat critical manifold, which allows the analysis to be reduced to a neighbourhood of the slow repelling manifold. This manifold is entirely contained in the region σ_L where the system is linear and, therefore, the transition map is just defined by a linear flow, which allows a good control of it. Despite the context specificity, it is expected that the relative position obtained between the transient canard, the maximum canard and the one flowing along the repelling slow manifold does not change after modifying the flat branch of the critical manifold to a non-zero slope segment. However, it is expected that the width of the interval in which the canard regime occurs, i.e. (x_r, x_s), tends to be finite as $\varepsilon \to 0$ and, therefore, the width of any of these cycles to be exponentially close. This could explain why it is so difficult to distinguish all these canard cycles in the smooth context when ε is small. Regarding the period function $T(x, \varepsilon)$, replacing the flat branch by a branch with a non-zero slope can alter the expression (33) and cause changes in both the number of existing critical (local maximum or minimum) periods and their location. This study is carried out in a work in progress.

6 Acknowledgments

VC is partially supported by Junta de Andalucía (Consejería de Economía, Conocimiento, Empresas y Universidad) projects P20-01160 and US-1380740, and by the Ministerio de Ciencia, Innovación y Universidade (MCIU) project PGC2018-096265-B-I00. SFG is partially supported by the MCIU project RTI2018-093521-B-C31. AET is partially supported by the MCIU project PID2020-118726GB-I00 and by the Ministerio de Economia y Competitividad through the project MTM2017-83568-P (AEI/ERDF,EU).

A About Poincaré maps

In the next result we summarize the time of flight expended by canard cycles Γ_x of width $x \in (x_r, x_s)$ in any of the linearity region, we also compute its derivative. In this result the time of flight, and its derivative, is referenced to the second coordinate, h, of the intersection point of the cycle Γ_x with the switching line $\{x = -\sqrt{\varepsilon}\}$ for headless canards, or the switching line $\{x = -1\}$ for canards with heads. To reference this time of flight to the width x of the cycle Γ_x we refer the reader to expression (9) just by considering $d = p_2 - h$.

Lemma A.1 *For $\varepsilon > 0$ and small enough let Γ_x be a limit cycle with $x \in (x_r, x_s)$. Let h be the second coordinate of the intersection point of Γ_x with the switching line $\{x = -\sqrt{\varepsilon}\}$ and located above the x-nullcline, if $x \in [-1, x_s)$, or with the switching line $\{x = -1\}$ and located under the x-nullcline, if $x \in (x_r, -1)$. It follows that*

$$\tau_R(h) = -\tfrac{1}{\lambda_R^s}\ln\left(\tfrac{(\lambda_R^q-\sqrt{\varepsilon})(\sqrt{\varepsilon}-a)-h}{(\lambda_R^q-\lambda_R^s)(\sqrt{\varepsilon}-a)}\right), \qquad \tau_R'(h) = \tfrac{1}{\lambda_R^s}\tfrac{1}{(\lambda_R^q-\sqrt{\varepsilon})(\sqrt{\varepsilon}-a)-h},$$

$$\tau_L(h) = \tfrac{1}{\lambda_L^s}\ln\left(\tfrac{(\lambda_L^q-\sqrt{\varepsilon})(\sqrt{\varepsilon}+a)+h}{(\lambda_L^q-\lambda_L^s)(\sqrt{\varepsilon}+a)}\right), \qquad \tau_L'(h) = \tfrac{1}{\lambda_L^s}\tfrac{1}{(\lambda_L^q-\sqrt{\varepsilon})(\sqrt{\varepsilon}+a)+h},$$

$$\tau_{Ld}(h) = \tfrac{1}{\lambda_L^s}\ln\left(\tfrac{(\lambda_L^q-\sqrt{\varepsilon})(\sqrt{\varepsilon}+a)+\lambda_L^s(\sqrt{\varepsilon}-1)+h}{(\lambda_L^q-\lambda_L^s)(\sqrt{\varepsilon}+a)}\right), \quad \tau_{Ld}'(h) = \tfrac{1}{\lambda_L^s}\tfrac{1}{(\lambda_L^q-\sqrt{\varepsilon})(\sqrt{\varepsilon}+a)+\lambda_L^s(\sqrt{\varepsilon}-1)+h}.$$

Proof: Next we obtain the expression of $\tau_R(h)$. For ε small enough, we obtain that Γ_x intersects the switching line $\{x = \sqrt{\varepsilon}\}$ above the x-nullcline at a point $\mathbf{p} = (\sqrt{\varepsilon}, h + O(\varepsilon^{\frac{3}{2}}))^T$. The order of the estimation of the second coordinate of $\mathbf{p}$ is a direct consequence of the monotonicity of the function providing the angle of the vector field along orbits in linear systems, see for instance Lemma 4.2.9 in [29]. Let $\varphi(t;\mathbf{p})$ be the solution of (1) with initial condition at $\mathbf{p}$. Thus, $\varphi(t;\mathbf{p}) \subset \sigma_R$ for $t \in [0, \tau_R(h)]$ and locally the solution can be written in terms of the eigenvalues λ_R^s, λ_R^q and the eigenvectors $\mathbf{v}_R^s$, $\mathbf{v}_R^q$ as follows

$$\varphi(t;\mathbf{p}) = \mathbf{e}_R + C_1 e^{\lambda_R^s t}\mathbf{v}_R^s + C_2 e^{\lambda_R^q t}\mathbf{v}_R^q, \quad t \in [0, \tau_R(h)], \tag{37}$$

where the constants

$$C_1 = \frac{(\lambda_R^q - \sqrt{\varepsilon})(\sqrt{\varepsilon} - a) - h}{\lambda_R^s(\lambda_R^q - \lambda_R^s)}, \quad C_2 = \frac{h - (\lambda_R^s - \sqrt{\varepsilon})(\sqrt{\varepsilon} - a)}{\lambda_R^q(\lambda_R^q - \lambda_R^s)},$$

are obtained from the equation $\varphi(0;\mathbf{p}) = \mathbf{p}$ by recalling that $\lambda_R^s + \lambda_R^q = -1$.

Assuming that $\varphi(\tau_R(h);\mathbf{p})$ is exponentially close to $\mathbf{q}_1^R$, we approximate the value of $\tau_R(h)$ from (37) as $\mathbf{q}_1^R = \mathbf{e}_R + C_1 e^{\lambda_R^s \tau_R(h)}\mathbf{v}_R^s$. More concretely, we obtain

$$\tau_R(h) = -\frac{1}{\lambda_R^s}\ln\left(\frac{|C_1|\|\mathbf{v}_R^s\|}{\|\mathbf{q}_1^R - \mathbf{e}_R\|}\right),$$

which provides the expression given in the statement. The derivative is straightforward obtained.

To compute the expression of $\tau_{Ld}(h)$ we consider the intersection point $\mathbf{p} = (-1, h)^T$ of Γ_x with $\{x = -1\}$ and located under the x-nullcline. Then, the solution through $\mathbf{p}$ can be locally written as

$$\varphi(t;\mathbf{p}) = \mathbf{e}_L + D_1 e^{\lambda_L^s t}\mathbf{v}_L^s + D_2 e^{\lambda_L^q t}\mathbf{v}_L^q, \quad t \in [-\tau_{Ld}(h), 0].$$

Assuming that $\varphi(-\tau_{Ld}(h);\mathbf{p})$ is exponentially close to $\mathbf{q}_1^L$, we conclude that $\mathbf{q}_1^L = \mathbf{e}_L + D_1 e^{-\lambda_L^s \tau_{Ld}(h)}\mathbf{v}_L^s$ what implies that

$$\tau_{Ld}(h) = \frac{1}{\lambda_L^s}\ln\left(\frac{|D_1|\|\mathbf{v}_L^s\|}{\|\mathbf{q}_1^L - \mathbf{e}_L\|}\right).$$

The result follows by using $\varphi(0;\mathbf{p}) = \mathbf{p}$ to compute D_1. Finally, the expression of $\tau_L(h)$ is obtained in a similar way. □

In the following result we present the time of flight and its derivative of Γ_x in the region σ_{LL} regardless of whether it is a canard cycle with head or a relaxation cycle.

Lemma A.2 *For $\varepsilon > 0$ and small enough let Γ_x be a limit cycle with $x < x_r$. Let h be the second coordinate of the intersection point of Γ_x with the switching line $\{x = -1\}$ and located under the x-nullcline. It follows that*

$$\tau_{LL}(h) = \tfrac{2}{\sqrt{\varepsilon}} \arctan\left(\tfrac{1-h+\sqrt{\varepsilon}(a-1)+\varepsilon}{\sqrt{\varepsilon}(1+a)}\right), \quad \tau'_{LL}(h) = -\tfrac{2(1+a)}{\varepsilon(1+a)^2+(1-h+\sqrt{\varepsilon}(a-1)+\varepsilon)^2},$$

and the expressions of $\tau_R(h)$ and $\tau'_R(h)$ are equal to the ones given in Lemma A.1.

Proof: Taking into account that the first component of the solution of system (1) in zone σ_{LL} with initial condition $(-1, h)$ is given by

$$x(t) = a - (1+a)\cos(\sqrt{\varepsilon}t) + \frac{h - (1+\sqrt{\varepsilon}(a-1)+\varepsilon)}{\sqrt{\varepsilon}}\sin(\sqrt{\varepsilon}t),$$

it is enough to make this expression equal to -1 and bear in mind that $1-\cos(\alpha) = \tan(\alpha/2)\sin(\alpha)$, for $\alpha \in (0, \pi/2)$.

The expressions of $\tau_R(h)$ and its derivative given in Lemma A.1 are also valid for the relaxation oscillations since, in such case, the cycle intersects $\{x = \sqrt{\varepsilon}\}$ exponentially close to $\mathbf{q}_1^R$. □

B Properties of function F in (26)

In this section we describe some qualitative and quantitative aspects of the function $F(x)$ given in (26), which is used in the proof of Lemma 4.1 and has been represented in Figure 7.

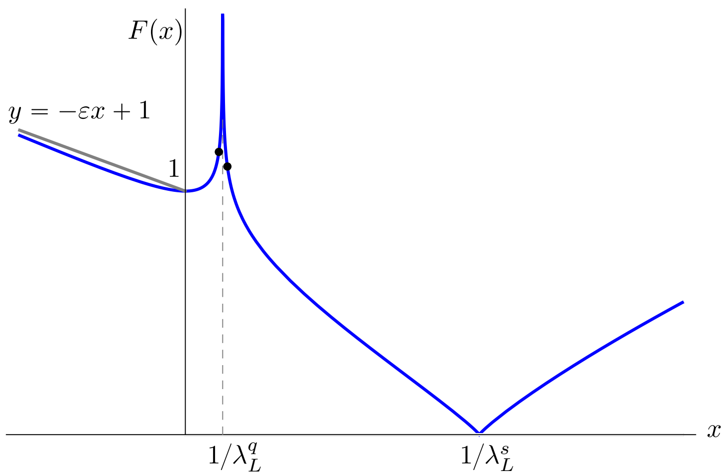

Figure 7: Representation of Function $F(x)$, its asymptotes and points $F(x_+)$ and $F(x_-)$.

The function $F(x)$ is continuous in the domain $\mathbb{D} = \mathbb{R}\backslash\{1/\lambda_L^q\}$, has a zero at $x = 1/\lambda_L^s$ and it is positive elsewhere, $F(x) > 0$ if $x \in \mathbb{D}\backslash\{1/\lambda_L^s\}$. Since

$$\lim_{x\nearrow 1/\lambda_L^q} F(x) = \lim_{x\searrow 1/\lambda_L^q} F(x) = +\infty, \tag{38}$$

the graph of $F(x)$ has a vertical asymptote at $x = 1/\lambda_L^q$ and a slant asymptote when $x \to -\infty$ in $y = -\varepsilon x + 1$. Moreover, the function is differentiable with continuity in $\mathbb{D}\backslash\{1/\lambda_L^s\}$, being

$$F'(x) = \frac{\varepsilon x(\lambda_L^q - \lambda_L^s)}{(1-x\lambda_L^q)(1-x\lambda_L^s)}F(x). \tag{39}$$

Note that the derivative vanishes at $x = 0$, which is a local minimum with $F(0) = 1$, and the local expression of $F(x)$ at the origin is

$$F(x) = 1 + (\lambda_L^q - \lambda_L^s)\varepsilon x^2 + O(x^3). \tag{40}$$

Furthermore, the derivative is strictly decreasing in $(1/\lambda_L^q, 1/\lambda_L^s)$ and strictly increasing in $(1/\lambda_L^s, +\infty)$, see Figure 7.

It is easy to check that, sufficiently close to $\frac{1}{\lambda_L^q}$, function F can be approximated by

$$F(x) \approx \frac{1}{|1 - \lambda_L^q x|^{\lambda_L^s}}$$

and therefore

$$x \approx \begin{cases} \frac{1}{\lambda_L^q} - \frac{1}{\lambda_L^q} e^{-\frac{1}{\lambda_L^s}\ln(F(x))}, & x < \frac{1}{\lambda_L^q}, \\ \frac{1}{\lambda_L^q} + \frac{1}{\lambda_L^q} e^{-\frac{1}{\lambda_L^s}\ln(F(x))}, & x > \frac{1}{\lambda_L^q}. \end{cases} \tag{41}$$

Finally, the behaviour of $F(x)$ with respect to ε satisfies that

$$F(x) = 1 - (x + \ln(1 - x))\varepsilon + O(\varepsilon^2), \tag{42}$$

what implies that for fixed $x \in \mathbb{D}$ it follows that $\lim_{\varepsilon \searrow 0} F(x) = 1$.

References

[1] E. Benoit, J.-L. Callot, F. Diener, et al, *Chasse au Canard.* Collect Math., **32**(1-2), 37–119, 1981.

[2] B.-W. Qin, K.-W. Chung, A. Algaba and A. J. Rodríguez-Luis, *High-order study of the canard explosion in an aircraft ground dynamics model*, Nonlinear Dynamics, **100**, 1079–1090, 2020.

[3] E. Bossolini, M. Brøns and K. U. Kristiansen, *Singular limit analysis of a model for earthquake faulting*, Nonlinearity, **30**, 2805–34, 2017.

[4] M. Brøns, M. Krupa and M. Wechselberger, *Mixed mode oscillations due to the generalized canard phenomenon.* Fields Inst. Comm., **49**, 39–63, 2006

[5] V. Carmona, S. Fernández-García and A. E. Teruel, *Saddle-node canard cycles in planar piecewise linear differential systems*, arXiv:2003.14112v2, 2020.

[6] V. Carmona and F. Fernández-Sánchez, *Integral characterization for Poincaré half-maps in planar linear systems*, arXiv:1910.13431, 2019.

[7] C. Chicone, *Bifurcations of Nonlinear Oscillations and Frequency Entrainment Near Resonance*, SIAM J. Math. Anal., **23**(6), 1577–1608, 1992.

[8] P. De Maesschalck, F. Dumortier, R. Roussarie,*Canard Cycles. From Birth to Transition*, A Series of Modern Surveys in Mathematics. Springer Nature Switzerland AG, 2021.

[9] M. Desroches, S. Fernández-García, M. Krupa, *Canards in a minimal piecewise-linear square-wave burster.*, Chaos, **26**, 2016.

[10] M. Desroches, S. Fernández-García, M. Krupa, R. Prohens and A. E. Teruel, *Piecewise-linear (PWL) canard dynamics: Simplifying singular perturbation theory in the canard regime using piecewise-linear systems*, Nonlinear Systems, Vol. 1 : Mathematical Theory and Computational Methods, Springer, 2018.

[11] M. Desroches, E. Freire, S. J. Hogan, E. Ponce and P. Thota *Canards in piecewise-linear systems: explosions and super-explosions*, Proceedings of the Royal Society A, **469**(2154), 20120603, 2013.

[12] M. Desroches and M. R. Jeffrey, *Canard and curvature: nonsmooth approximation by pinching* Nonlinearity, **24**(5), 1655–1682, 2011.

[13] M. Desroches, J. Guckenheimer, B. Krauskopf, C. Kuehn, H. M. Osinga and M. Wechselberger, *Mixed-mode oscillations with multiple time scales.* SIAM Review **54**(2), 211–288, 2012.

[14] M. Desroches, A. Guillamon, E. Ponce, R. Prohens, S. Rodrigues and A. E. Teruel,*Canards, folded nodes and mixed-mode oscillations in piecewise-linear slow-fast systems.* SIAM Review, **58**(4), 653–691, 2016.

[15] M. Desroches, M. Krupa and S. Rodrigues, *Inflection, canards and excitability threshold in neuronal models*, J. Math. Biol., **67**, 989–1017, 2013.

[16] F. Dumortier and R. Roussarie, *Canard cycles and center manifolds*, **121**, Providence (RI):AMS, 1996.

[17] N. Fenichel, *Geometric singular perturbation theory for ordinary differential equations*, J. Differ. Equations, **31**(1), 53–98, 1979.

[18] S. Fernández-García , M. Desroches, M. Krupa and A. E. Teruel, *Canard solutions in planar piecewise linear systems with three zones*, Dynam. Syst., **31**(2), 173–197, 2016.

[19] R. FitzHugh, *Impulses and physiological states in theoretical models of nerve membrane*, Biophys. J., **1**, 445–466, 1961.

[20] E. Freire, E. Ponce, and F. Torres, *Hopf-like bifurcations in planar piecewise linear systems*, Publicacions Matemàtiques, 41 (1997), pp. 135–148, https://doi.org/10.5565/PUBLMAT 41197 08.

[21] E. Freire, E. Ponce, F. Rodrigo and F. Torres, *Bifurcation Sets of Continuous Piecewise Linear Systems with Two Zones*, Internat. J. Bifur. Chaos Appl. Sci. Engrg., **8**(11), 2073–2097, 1998.

[22] I. Gucwa and P. Szmolyan, *Geometric singular perturbation analysis of an autocatalator model*, Discrete Contin. Dynam. Syst. Ser. S, **2**(4), 783–806, 2009.

[23] M. Krupa and P. Szmolyan, *Relaxation Oscillation and Canard Explosion,* Journal of Differential Equations, **174**, 312–368, 2001.

[24] K. U. Kristiansen, *Blowup for flat slow manifolds*, Nonlinearity, **30**, 2138–2184, 2017.

[25] C. Kuehn, *Normal hyperbolicity and unbounded critical manifolds*, Nonlinearity, **27**, 1351, 2014.

[26] J. Llibre, E. Nuñez and A.E. Teruel, *Limit cycles for planar piecewise linear differential systems via first integrals*, Qualitative Theory of Dynamical Systems, **3**, 29–50, 2002.

[27] P. De Maesschalck, F. Dumortier and R. Roussarie, *Canard cycle transition at a slow-fast passage through a jump point*, Comptes Rendus Mathematique, **352**, 317–320, 2014.

[28] J. Nagumo, S. Arimoto and S. Yoshizawa, *An active pulse transmission line simulating nerve axon*, Proceedings of the IRE, **50**, 2061–2070, 1962.

[29] J. Llibre and A. E. Teruel, *Introduction to the Qualitative Theory of Differential Systems: Planar, Symmetric and Continuous Piecewise Linear Systems*, Springer Basel, Birkhäuser Advanced Texts Basler Lehrbücher, Basel, 2014.

[30] I. Ortega-Piwonka,A.E. Teruel, R. Prohens, C. Vich and J. Javaloyes *Simplified description of dynamics in neuromorphic resonant tunneling diodes.* Chaos: An Interdisciplinary Journal of Nonlinear Science, 31(11), 113128, 2021.

[31] R. Prohens, A.E. Teruel and C. Vich, *Slow–fast n-dimensional piecewise linear differential systems*, Journal of Differential Equations, **260**, 1865–1892, 2016.

[32] J. Rankin, M. Desroches, B. Krauskopf and M. Lowenberg, *Canard cycles in aircraft ground dynamics*, Nonlinear Dyn., **66**, 681–688, 2011.

[33] J. Rinzel, *A formal classification of bursting mechanisms in excitable systems*. International Congress of Mathematicians, Berkeley, California, USA, August 3-11, 1986, **II**, 1578–1593. American Mathematical Society, 1987.

[34] H.G. Rotstein, S. Coombes, and A.M. Gheorghe: *Canard-like explosion of limit cycles in two-dimensional piecewise-linear models of FitzHugh-Nagumo type*. SIAM J.Appl. Dyn. Syst. 11(1), 135–180 (2012)

[35] D. J. W. Simpson, *A compendium of Hopf-like bifurcations in piecewise-smooth dynamical systems*, Physics Letters A, **382**, 2439-2444, 2018.

[36] D. J. W. Simpson,*Twenty Hopf-like bifurcations in piecewise-smooth dynamical systems*, arXiv, 2019.

[37] M. Wechselberger, *Geometric Singular Perturbation Theory Beyond the Standard Form*, Springer Nature Switzerland AG, 2020.

[38] M. Wechselberger, J. Mitry, and J. Rinzel, *Canard Theory and Excitability*, in Nonautonomous Dynamical Systems in the Life Sciences, Springer International Publishing, 89–132, 2013.

[39] J. Mitry, M. McCarthy, N. Kopell and M. Wechselberger, *Excitable Neurons, Firing Threshold Manifolds and Canards*, Journal of Mathematical Neuroscience, **3**(12), 1–32, 2013.

[40] M. Wechselberger, *A Propos de Canards*. Transactions of the American Mathematical Society, **364**(6), 3289–3309, 2012.